

28. CONVENTIONAL AND $^{40}\text{Ar}/^{39}\text{Ar}$ K-AR AGES OF VOLCANIC ROCKS FROM ŌJIN (SITE 430), NINTOKU (SITE 432), AND SUIKO (SITE 433) SEAMOUNTS AND THE CHRONOLOGY OF VOLCANIC PROPAGATION ALONG THE HAWAIIAN-EMPEROR CHAIN

G. Brent Dalrymple and Marvin A. Lanphere, U.S. Geological Survey, Menlo Park, California
and

David A. Clague, Department of Geology, Middlebury College, Middlebury, Vermont

ABSTRACT

Conventional K-Ar, $^{40}\text{Ar}/^{39}\text{Ar}$ total fusion, and $^{40}\text{Ar}/^{39}\text{Ar}$ incremental heating data on hawaiite and tholeiitic basalt samples from Ōjin (Site 430), alkalic basalt samples from Nintoku (Site 432), and alkalic and tholeiitic basalt samples from Suiko (Site 433) seamounts in the Emperor Seamount chain give the following best ages for these volcanoes: Ōjin = 55.2 ± 0.7 m.y., Nintoku = 56.2 ± 0.6 m.y., and Suiko = 64.7 ± 1.1 m.y. These new data bring to 27 the number of dated volcanoes in the Hawaiian-Emperor volcanic chain. The new dates prove that the age progression from Kilauea Volcano on Hawaii (0 m.y.) through the Hawaiian-Emperor bend (~ 43 m.y.) to Kōkō Seamount (48.1 m.y.) in the southernmost Emperor Seamounts continues more than halfway up the Emperor chain to Suiko Seamount.

The age versus distance data for the Hawaiian-Emperor chain are consistent with the kinematic hot-spot hypothesis, which predicts that the volcanoes are progressively older west and north away from the active volcanoes of Kilauea and Mauna Loa. The data are consistent with an average volcanic propagation velocity of either 8 cm/year from Suiko to Kilauea or of 6 cm/year from Suiko to Midway followed by a velocity of 9 cm/year from Midway to Kilauea, but it appears that the change in direction that formed the Hawaiian-Emperor bend probably was not accompanied by a major change in velocity.

INTRODUCTION

One of the more interesting ideas to arise from sea-floor spreading and plate tectonic theory is the hot-spot hypothesis. In its most general and purely kinematic form, this hypothesis states that linear volcanic island chains originate as a crustal plate moves relative to a source of lava in the asthenosphere. Each volcano in the chain forms above the hot spot, is eventually moved away from its source, and a new volcano is erupted onto the sea floor behind it. First proposed by Wilson (1963a, b) to explain the origin of the Hawaiian Islands and other parallel northwest-southeast island chains in the Pacific, the idea was later extended by Christofferson (1968), who coined the term "hot spot," to include the Emperor Seamounts as a northward extension of the Hawaiian chain. According to Christofferson, the Hawaiian-Emperor bend represents a major change in sea-floor spreading direction from northward to westward. The hot-spot hypothesis was more fully developed by Morgan (1972a, b), who proposed that hot spots were narrow plumes of material rising from the deep mantle, were fixed relative to one another, and provided the driving force for plate motion.

One of the most important corollaries of the hot-spot hypothesis is that the volcanoes in a linear island chain should progressively increase in age from one end to the other. Although age versus distance relationships provide little or no information about hot-spot mechanisms or hot-spot fixity, they do provide a direct test of the kinematics and thus a critical test of the general hot-spot hypothesis. Indeed, it was the (then poorly known) age progression in the Hawaiian Islands that led Wilson (1963b) to propose his imaginative hypothesis.

Because of accessibility and the amount of geologic work done through the years in the Hawaiian Islands, the Hawaiian-Emperor chain is the most promising site for a definitive age-dating experiment to test the kinematic hot-spot hypothesis. Although some age versus distance data have been obtained for several other linear island chains in the Pacific (see summaries in Jackson, 1976; Jarrard and Clague, 1977), the structure, petrology, and eruptive sequence of non-Hawaiian Pacific volcanoes are not well known and the age data from these other island chains are not easily interpreted.

It has been known since the pioneering work of Dana (1849, 1890) that the Hawaiian Islands become geomorphically more mature westward from the active vol-

canoes of Mauna Loa and Kilauea on the island of Hawaii (see also Wentworth, 1927; Hinds, 1931; Stearns, 1946). The first K–Ar radiometric data for the Hawaiian Islands became available with the work of McDougall (1963, 1964), who showed that the shield volcanoes that form the five principal Hawaiian Islands are progressively older from Hawaii (<1 m.y.) to Kauai (3.8 to 5.6 m.y.). Subsequent K–Ar studies have augmented the work of McDougall in the main Hawaiian Islands (Funkhouser et al., 1968; Dalrymple, 1971; Gramlich et al., 1971; McDougall and Swanson, 1972; Doell and Dalrymple, 1973; Bonhommet et al., 1977), and have extended the age data to half of the Leeward Hawaiian Islands (Dalrymple et al., 1974, 1977), to several seamounts in the western Hawaiian chain (Clague et al., 1975), and to the southernmost Emperor Seamounts (Clague and Dalrymple, 1973; Clague et al., 1975; Dalrymple and Clague, 1976). These new data have conclusively shown that the age progression continues westward beyond Kauai, around the Hawaiian–Emperor bend (43 m.y.) and as far as Kōkō Seamount (48 m.y.) 200 km north of the bend (Figure 1).

Until Leg 55 (also Dalrymple and Garcia, this volume), data from the seamounts north of Koko have been insufficient to adequately test the hypothesized age progression for the Emperor Seamount chain. DSDP Hole 192A (Leg 19) recovered lower Maestrichtian (70 to 72 m.y.) nanoflora (Worsley, 1973) above basalt on Meiji Seamount (Figure 1), but the basalt is extensively altered and gives only a minimum K–Ar age of 61.9 ±

5.0 m.y. (Dalrymple et al., this volume). In addition, the Emperor chain may bend eastward toward the Aleutian Trench and Meiji may not be an Emperor volcano (Jackson et al., 1972). The only other data are from Suiko Seamount. These include a $^{40}\text{Ar}/^{39}\text{Ar}$ isochron age of 59.6 ± 0.6 m.y. on a dredged mugearite (Saito and Ozima, 1975, 1977) and three conventional K–Ar ages ranging from 21.8 to 42.9 m.y. on dredged andesite and basalt (Ozima et al., 1970). The andesite and basalt samples, however, may be ice-rafted (Ozima et al., 1970) and, as discussed later in this paper, there is also reason to suspect the reliability of the $^{40}\text{Ar}/^{39}\text{Ar}$ age on the mugearite.

The purpose of the study reported in this paper was to test the age progression predicted by the hot-spot hypothesis for the Emperor Seamount chain by determining the radiometric ages of volcanic rocks recovered on Leg 55 from Ōjin, Nintoku, and Suiko Seamounts.

Four sites in the Emperor Seamounts were drilled during Leg 55 (Figure 1). These included single-bit holes on Ōjin (Site 430), Yōmei (Site 431), and Nintoku (Site 432), and a multiple re-entry hole on Suiko (Site 433). The two holes at Site 431 bottomed in sediments, but holes on Ōjin, Nintoku, and Suiko reached subaerially erupted lava flows petrographically and chemically similar to the lava flows that form the main Hawaiian Islands (Kirkpatrick et al., this volume).

Hole 430A on Ōjin Seamount penetrated 59.3 meters of sediment and 58.7 meters of lava flows (Figure 2), including four flows of hawaiite (Flow Units 1 through 4) underlain by a flow of tholeiitic basalt (Flow Unit 5). The sediments consist primarily of calcareous ooze and sand interbedded near the base with 12 meters of volcanoclastic sand. These sediments contain benthic foraminifers, ostracodes, and calcareous algae indicative of a shallow-water reef or bank environment. The oldest sediments contain lower Eocene to upper Paleocene foraminifers and upper Paleocene nanofossils.

Hole 432A on Nintoku Seamount penetrated three flows (Flow Units 1 through 3) of alkalic basalt, beginning at a sub-bottom depth of 42.1 meters and totaling 31.9 meters in thickness. The sediments above the basalt consist of fossiliferous volcanic sandstone and calcareous conglomerate with clasts of alkalic basalt, hawaiite, and mugearite, and fragments of calcareous algae, shells, and bryozoans indicating a shallow-water reef or bank environment. The limited fossil assemblage indicates that the oldest sediments above the basalt are Paleocene.

Hole 433C on Suiko Seamount reached a sub-bottom depth of 550.5 meters after penetrating 387.5 meters of lava flows overlain by 163.0 meters of sediments. The volcanic rocks consist of three flows (Flow Units 1 through 3) of alkalic basalt underlain by more than 90 flows (Flow Units 4 through 67) of tholeiitic basalt. The uppermost 52 meters of sediments consist primarily of pelagic oozes, ranging from Pleistocene to lower Miocene. These are underlain by middle Paleocene carbonate sands, sandy muds, and calcarenites that contain shallow-water reef fossils including benthic foraminifers, calcareous algae, bryozoans, and ostracodes. Four

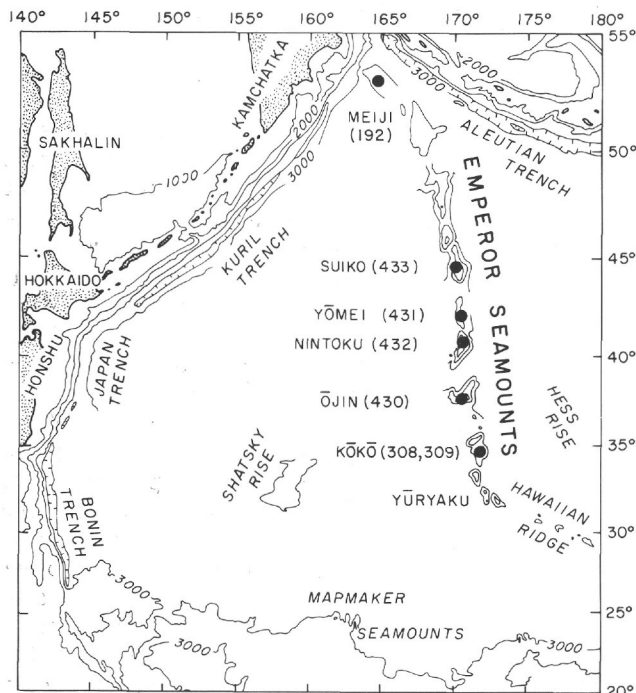


Figure 1. Index chart of the northwest Pacific Ocean, showing locations of DSDP Leg 55 drilling sites in the Emperor Seamounts. Datable volcanic rock was recovered from Sites 430, 432, and 433.

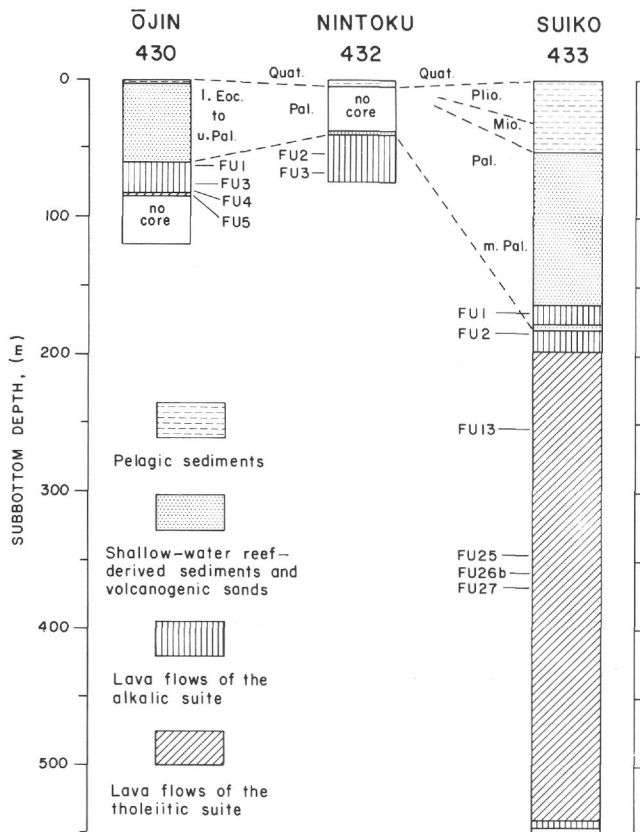


Figure 2. Generalized stratigraphy at DSDP Sites 430, 432, and 433, showing positions of flow units (FU) analyzed for conventional K-Ar and $^{40}\text{Ar}/^{39}\text{Ar}$ dating.

meters of reef carbonate sand containing volcanoclastic material was also found between Flow Units 1 and 2.

SAMPLES STUDIED

Nearly all the basalts recovered on Leg 55 are altered, and only a few meet the usual criteria for whole-rock K-Ar dating (Mankinen and Dalrymple, 1972). A few additional flows are only slightly altered, but most are moderately to very highly altered and contain clays of the montmorillonite group as interstitial fillings, as large irregular and spherical replacement patches in the groundmass, and as replacements for olivine, plagioclase, and pyroxene (Kirkpatrick et al., this volume; Avdeiko et al., this volume). In an electron microprobe study of similar clays in samples from three seamounts near the Hawaiian-Emperor bend, Dalrymple and Clague (1976) showed that the clays can contain more than 5 weight per cent K_2O . Such clays adversely affect the conventional K-Ar ages, but if the clays are not too abundant, a reliable age may be obtained by $^{40}\text{Ar}/^{39}\text{Ar}$ techniques.

For the present study, 204 thin sections from 65 flow units were examined. The 17 least altered samples from 12 flow units from Ōjin (4 flow units), Nintoku (2 flow units), and Suiko (6 flow units) were selected for conventional K-Ar and $^{40}\text{Ar}/^{39}\text{Ar}$ dating. The relative stra-

tigraphic positions of the analyzed samples are shown in Figure 2 and the alteration summarized in Table 1.

Brief sample descriptions follow and the alteration and other petrographic information which could adversely affect the K-Ar determinations are noted in Table 1. More detailed petrography and geochemistry of these same samples are presented by Kirkpatrick et al. (this volume), and microprobe analyses of the primary mineral phases are presented by Clague and Fisk (this volume). The rock names used here are based on petrographic and geochemical data from the shipboard examination and from Kirkpatrick et al. (this volume).

The studied samples from Hole 430A include four hawaiites from Flow Units 1 to 4 and the tholeiitic basalt of Flow Unit 5. Sample 430A-4-2, 110–118 cm is a massive hawaiite with subtrachytic texture and intergranular clinopyroxene. Sample 430A-5-1, 21–27 cm is a massive hawaiite with trachytic texture and sub-ophitic clinopyroxene; it also contains rare plagioclase microphenocrysts. Sample 430A-6-3, 52–63 cm is a massive hawaiite with trachytic texture and intergranular clinopyroxene; it contains rare titanomagnetite microphenocrysts. Sample 430A-6-4, 7–15 cm is a massive hawaiite with subtrachytic texture and rare intergranular clinopyroxene; it contains rare olivine microphenocrysts and partly resorbed plagioclase microphenocrysts. Sample 430A-6-4, 140–150 cm is a massive glomeroporphyritic tholeiitic basalt with intergranular texture and phenocrysts of plagioclase, augite, and olivine.

The three studied samples from Hole 432A are alkalic basalts from Flow Units 2 and 3. Sample 432A-2-3, 37–43 cm is a massive porphyritic alkali basalt with diabasic texture and phenocrysts of plagioclase and olivine. The groundmass clinopyroxene is a pale purple-brown titanaugite. Sample 432A-3-2, 120–126 cm is a massive fine-grained sparsely porphyritic alkali basalt that contains rare olivine and plagioclase microphenocrysts. Sample 432A-5-2, 57–66 cm is a massive sparsely porphyritic alkali basalt with ophitic texture and rare microphenocrysts of olivine and plagioclase.

The studied samples from Site 433 include three samples of Flow Unit 1, two from Flow Unit 13, and one each from Flow Units 2, 25, 26b, and 27. Samples 433A-20-1, 30–36 cm, 433A-21-4, 129–138 cm, and 433B-5-2, 61–68 cm are all massive porphyritic alkali basalts containing phenocrysts of sector-zoned augite, plagioclase, and olivine. Sample 433A-21-4, 129–138 cm is distinct in that the rock is glomeroporphyritic. Sample 433C-4-1, 25–28 cm is also a massive porphyritic alkali basalt, but it is distinct from the Flow Unit 1 samples in that the pyroxenes are only rarely sector-zoned, olivine is more abundant and still generally unaltered, and some of the olivine shows kink bands and is interpreted to be xenocrystic. Sample 433C-15-6, 16–31 cm is a massive plagioclase and olivine microporphyritic tholeiitic basalt. Sample 433C-17-1, 78–82 cm is a massive sparsely porphyritic tholeiitic basalt containing phenocrysts of plagioclase, olivine, and augite. Sample 433C-28-2, 73–80 cm is a massive porphyritic tholeiitic basalt con-

TABLE 1
Alteration Summary and Relative Suitability, Based on Petrographic Examinations, for K-Ar Dating of Analyzed Samples from Ōjin (Site 430), Nintoku (Site 432), and Suiko (Site 433) Seamounts

Flow Unit	Hole	Core-Section, Interval (cm)	Rock Type	Rank ^a	Clays (%)	Remarks
ŌJIN SEAMOUNT						
1	430A	4-2, 110-118	Hawaiite	4	19	Olivine replaced by iddingsite, interstitial brown clays.
1	430A	5-1, 21-27	Hawaiite	2	7	Olivine replaced by brown clays, interstitial brown clays.
3	430A	6-3, 52-63	Hawaiite	4	16	Olivine replaced by brown clays, interstitial green-brown clays.
4	430A	6-4, 7-15	Hawaiite	4	17	Olivine replaced by brown clays, interstitial green-brown clays occasionally fill vesicles.
5	430A	6-4, 140-150	Tholeiitic basalt	2	3	Olivine replaced by brown clays, occasional clay-filled vesicles.
NINTOKU SEAMOUNT						
2	432A	2-3, 37-43	Alkalic basalt	2	6	Olivine replaced by iddingsite, interstitial yellow-brown clays, rare calcite.
3	432A	3-2, 120-126	Alkalic basalt	1	1	Olivine partly replaced by brown clays.
3	432A	5-2, 57-66	Alkalic basalt	3	2	Olivine partly replaced by brown clays, interstitial green-brown clays.
SUIKO SEAMOUNT						
1	433A	20-1, 30-36	Alkalic basalt	3	9	Olivine replaced by brown clays and rare calcite, interstitial yellow-brown clays, plagioclase has colorless clays along fractures, fracture in rock has hematite.
1	433A	21-4, 129-138	Alkalic basalt	3	11	Olivine replaced by pleochroic green-brown clays, rare vesicles filled with brown clays and rare calcite.
1	433B	5-2, 61-68	Alkalic basalt	3	9	Olivine replaced by brown clays, interstitial brown clays, plagioclase has colorless clays along fractures.
2	433C	4-1, 25-28	Alkalic basalt	3	10	Olivine replaced by fibrous yellow-brown clays, interstitial greenish clays.
13	433C	15-6, 16-31	Tholeiitic basalt	2	8	Interstitial brown clays, some in rounded pools.
13	433C	17-1, 78-82	Tholeiitic basalt	1	2	Olivine replaced by dark brown clays, rare interstitial dark brown clay.
25	433C	28-2, 73-80	Tholeiitic basalt	3	5	Interstitial brown clays, rare vesicles filled with pale brown clays.
26b	433C	29-2, 94-100	Tholeiitic basalt	4	12	Botryoidal greenish interstitial clays, olivine replaced with iddingsite rim filled by green and pale brown clays; plagioclase has colorless clays along fractures.
27	433C	31-1, 7-13	Tholeiitic basalt	2	3	Olivine is partly replaced by brown clays along fractures, interstitial bright green clays; plagioclase cores partially replaced by bright green clays.

^aRelative suitability for dating:

- 1) Appear to meet normal criteria for K-Ar dating, virtually unaltered.
- 2) Slightly altered.
- 3) Slightly to moderately altered.
- 4) Moderately altered.

taining phenocrysts of plagioclase and augite. Sample 433C-29-2, 94-100 cm is a massive sparsely porphyritic tholeiitic basalt containing phenocrysts of plagioclase, olivine, and augite. Sample 433C-31-1, 7-13 cm is a massive porphyritic tholeiitic basalt containing phenocrysts of olivine and plagioclase.

Electron microprobe analyses of the clays in 10 of the dated samples (Table 2) show that the clays have relatively low K₂O contents. Nearly all the clays analyzed are Fe-rich saponite. The data in Table 2 are not as high quality as normal microprobe analyses, for several reasons: the surface of the clays does not polish well, no matrix correction for the water present has been applied, and the standards used are not very close in composition to the analyzed clays. In particular, the SiO₂ values obtained are fairly erratic because of difficulties focusing the beam on the unpolished clay surface. This

mainly affects SiO₂, because it has a very low incidence angle on the diffracting crystal and is therefore highly sensitive to beam focus.

All the clays analyzed are very low in CaO and TiO₂ contents. Whereas K₂O contents in clays from samples recovered from seamounts on the Hawaiian-Emperor bend were usually greater than 1 per cent (Dalrymple and Clague, 1976), all but four of the analyzed clays in the Leg 55 samples contain much less than 1 per cent K₂O. In most montmorillonite clays, Ca is the dominant exchangeable cation; in the analyzed samples, Na is always the main exchangeable cation.

Volume calculations indicate that the greater part of the K₂O in the dated samples resides in primary igneous phases rather than in the secondary clays. We estimate that the maximum proportion of K₂O in secondary clays relative to the proportion in the whole rock is about 7 to

TABLE 2

Summary of Electron Microprobe Analyses of Clay Minerals in Selected Samples Used for Conventional K-Ar and $^{40}\text{Ar}/^{39}\text{Ar}$ Dating Experiments (Range and median values are given.)

Hole	ŌJIN						NINTOKU		SUIKO			
	430A	430A	430A	430A	430A	430A	432A	432A	433A	433B	433C	433C
Core-Section	4-2	6-3	6-4	6-4	6-4	6-4	3-2	5-2	21-4	5-2	15-6	28-2
Interval (cm)	100-118	52-63	7-15	7-15	140-150	140-150	120-126	57-66	129-138	61-68	16-31	73-80
Material	Clay	Clay	Clay	Clay	Iddingsite	Clay						
Occurrence ^a	i.	i.	r.b.	i.	a.o.	i.						
No. of Analyses	9	6	3	6	4	5	5	6	7	6	6	7
Flow Unit	1	3	4	4	5	5	3	3	1	1	13	25
SiO ₂	44.5 44-45	34.5 34-39	43.0 43-45	38.0 36-40	49.0 48-50	47.0 46-49	47.2 45-49	38.8 37-45	38.6 37-40	40.2 36-43	45.1 43-48	45.9 44-47
Al ₂ O ₃	5.3 4.8-11.2	8.5 5.8-9.3	5.6 4.6-5.9	8.8 7.3-9.5	3.9 3.3-4.1	4.5 3.5-5.8	4.0 3.6-4.1	6.4 3.6-8.8	6.7 5.8-7.6	5.3 5.0-7.2	6.3 3.7-7.5	4.3 4.1-6.1
FeO	14.0 10.6-24.8	21.8 21.2-28.5	17.0 15.4-17.5	22.2 20.7-22.6	21.0 18.2-21.2	20.6 17.0-22.4	18.1 15.9-22.5	21.0 18.8-23.6	23.9 21.6-26.3	18.3 17.3-23.2	15.5 14.9-17.5	15.4 12.0-16.6
MgO	14.1 4.2-16.8	16.0 12.8-17.8	17.6 17.3-18.0	17.2 16.4-18.2	14.5 14.2-16.0	13.0 10.4-14.5	14.2 11.8-19.2	15.6 14.6-16.8	13.4 10.8-13.9	12.4 11.2-14.2	14.2 12.2-17.1	15.3 12.6-16.7
CaO	0.02 .00-2.0	.14 .11-.35	.05 .02-.06	.15 .11-.22	.28 .22-.29	.34 .13-1.1	.20 .07-1.9	.19 .16-.24	.16 .10-.21	.08 .05-.5.4	.29 1.5-1.2	.48 .35-.64
Na ₂ O	1.2 .80-1.8	1.3 1.2-1.7	1.36 1.3-1.5	1.1 .42-1.5	1.8 1.5-1.8	1.6 1.1-1.7	1.1 .68-2.2	1.2 1.0-1.5	1.7 1.4-1.9	1.8 1.6-2.4	2.24 1.3-2.7	1.73 1.6-2.2
K ₂ O	0.67 .28-3.1	.21 .13-.38	1.1 .86-1.4	.07 .02-.27	.59 .55-.61	.58 .50-.88	.65 .51-.77	.18 .15-.59	.17 .04-.22	.34 .24-.48	.09 .07-.16	.14 .08-.30
TiO ₂	0.13 .02-.83	.10 .06-.48	.02 .00-.02	.06 .04-.20	.08 .02-.11	.15 .10-.33	.07 .04-.11	.14 .09-.18	.14 .06-.31	.12 .04-.23	.17 .14-.45	.34 .25-.53

^ai. = interstitial, r.b. = round balls, a.o. = after olivine.

10 per cent, with the possible exception of Sample 433C-29-2, 94-100 cm, which may have a considerably higher percentage of K₂O in the clays.

TECHNIQUES

Samples for both conventional Ar and $^{40}\text{Ar}/^{39}\text{Ar}$ analyses were small cores 6 mm in diameter and 1 cm long, taken from the same intervals as the rock powders used for several other types of shorebased analyses. After the K-Ar cores and the thin-section slabs were cut, the remainder of the sample was pulverized and used for analysis of major oxide and trace elements (Kirkpatrick et al., this volume), rare-earth elements (Clague and Frey, this volume), and Sr isotopic composition (Lanphere et al., this volume), as well as for K₂O measurements for the conventional K-Ar ages (Table 3).

K₂O measurements were made in duplicate on two separate splits of each sample powder (four measurements total) by flame photometry after lithium metaborate fusion and dissolution (Ingamells, 1970). Argon analyses were by isotope-dilution mass spectrometry using a high-purity (>99.9%) ^{38}Ar tracer and techniques and equipment previously described (Dalrymple and Lanphere, 1969). All samples for Ar extraction, including those for $^{40}\text{Ar}/^{39}\text{Ar}$ analyses, were baked overnight in vacuum in the extraction system at 280°C. Isotope-dilution Ar mass analyses were done on a computerized multiple collector mass spectrometer with 22.86 cm radius and a nominal 90° sector magnet (Stacey et al., 1978; Sherrill and Dalrymple, in press).

Samples for $^{40}\text{Ar}/^{39}\text{Ar}$ dating were sealed in air in flat-bottomed, fused silica vials and irradiated at 1

megawatt in the core of the U.S. Geological Survey TRIGA reactor for from 30 to 40 hours, where they received a neutron dose of approximately $3-4 \times 10^{18}$ nvt. The samples were irradiated in levels, each level containing two biotite flux monitors and five unknown samples, all held in precisely the same vertical alignment by a machined sample rack. The samples on each level were arranged in hexagonal symmetry, with one monitor in the center and the other monitor and the five unknowns in an outer ring. The diameter of the ring is about 0.9 cm. Statistical analysis of the results of measurements on 47 pairs of monitors irradiated during the past six years gives a pooled estimate of the standard deviation of precision of 0.8 per cent. Further details of the reactor flux characteristics, the monitor mineral, and the corrections for interfering K- and Ca-derived Ar isotopes are given in Dalrymple and Lanphere (1971), and Dalrymple et al. (in press).

Irradiated samples were fused by induction heating and the Ar purified in a standard Ar extraction line. Temperatures for $^{40}\text{Ar}/^{39}\text{Ar}$ incremental heating experiments were measured with a platinum/platinum-rhodium thermocouple inserted into a small hole in the bottom of a machined molybdenum crucible, and are accurate to within about $\pm 20^\circ\text{C}$ (Lanphere and Dalrymple, 1971). The samples were held for 30 minutes at each temperature. Ar analyses for the $^{40}\text{Ar}/^{39}\text{Ar}$ experiments were done with a Nier-type, 15.24-cm-radius, 60°-sector-magnet, single-collector mass spectrometer utilizing analog data acquisition.

Errors given for the calculated ages of individual measurements are estimates of the standard deviation of analytical precision. These were calculated using for-

TABLE 3
Conventional and ⁴⁰Ar/³⁹Ar Total Fusion Age Data on Samples from DSDP Leg 55, Sites 430, 432, and 433

Hole	Core-Section, Interval (cm)	Flow Unit	Rock Type	K ₂ O (wt. %)	Argon ^a		Calculated Age (10 ⁶ years) ^b	J	40Ar/ ³⁹ Ar	37Ar/ ³⁹ Ar ^c	36Ar/ ³⁹ Ar	36Ar/ ^{Ca} (%)	39Ar/ ^{Ca} (%)	40Ar/ ^K (%)	40Ar (%)	Calculated Age (10 ⁶ years) ^b
					Weight (g)	40Ar (mol/g)										
					40Ar (mol/g)	40Ar (%)										
OJIN SEAMOUNT																
430A	4-2, 110-118	1	Hawaiite	1.930±0.004	0.6838	1.552 × 10 ⁻¹⁰	81.6	0.006608	9.229	1.378	0.01492	2.5	<0.1	<0.1	53.4	57.8±1.1
	5-1, 21-27	1	Hawaiite	1.682±0.005	0.6164	1.269	44.1	0.009584	5.879	1.791	0.00859	5.6	0.1	0.1	59.2	59.3±1.0
	6-3, 52-63	3	Hawaiite	1.696±0.018	0.6898	1.273	62.8	0.006743	5.310	1.708	0.00236	19.7	0.1	0.1	89.3	56.8±0.8
	6-4, 7-15	4	Hawaiite	1.596±0.001	0.7171	1.282	71.7	0.006608	8.856	1.984	0.003945	13.7	0.1	0.1	82.7	56.9±0.8
	6-4, 140-150	5	Tholeiite	0.382±0.000	0.7858	0.2543	32.0	0.009063	10.25	1.877	0.01219	4.2	0.1	0.1	58.5	57.2±1.0
								0.009063	10.25	12.67	0.02727	12.6	0.8	<0.1	31.2	52.0±1.7
NINTOKU SEAMOUNT																
432A	2-3, 37-43	2	Alkalic basalt	1.420±0.002	lost	lost	31.6	0.009063	4.717	3.698	0.00507	19.8	0.2	0.1	74.4	56.6±0.8
	3-2, 120-126	3	Alkalic basalt	1.124±0.002	0.6898	0.8855	54.0	0.009584	5.783	3.130	0.00974	8.7	0.2	0.1	54.5	53.8±1.0
	3-2, 57-66	3	Alkalic basalt	1.064±0.005	0.7594	0.8386	54.0	0.006608	6.482	3.344	0.00694	13.1	0.2	0.1	72.4	55.2±0.8
SUIKO SEAMOUNT																
433A	20-1, 30-36	1	Alkalic basalt	0.934±0.003	0.7352	0.8059	36.1	0.009063	8.382	4.07	0.0168	6.6	0.3	<0.1	44.6	60.2±1.3
433B	21-4, 129-138	1	Alkalic basalt	0.919±0.002	0.7326	0.8505	62.0	0.006608	6.969	4.62	0.00698	18.0	0.3	<0.1	75.6	62.0±0.9
433C	5-2, 61-68	1	Alkalic basalt	0.876±0.001	0.7453	0.7584	36.7	0.009584	5.463	5.14	0.00788	17.7	0.3	0.1	64.8	60.4±0.9
	4-1, 25-28	2	Alkalic basalt	0.795±0.003	0.8026	0.7132	32.8	0.008220	12.09	5.28	0.02830	5.08	0.3	<0.1	34.3	60.7±1.6
	15-6, 16-31	13	Tholeiite	0.282±0.003	0.6781	nil	0	0.009068	19.36	26.30	0.0618	11.6	1.7	<0.1	16.5	52.5±3.5
	17-1, 78-82	13	Tholeiite	0.316±0.002	0.8215	0.2177	36.0	0.008220	9.263	16.80	0.02258	20.2	1.1	<0.1	42.5	58.0±1.4
	28-2, 73-80	25	Tholeiite	0.182±0.001	0.7681	0.0949	20.7	0.009063	24.47	33.45	0.0825	11.0	2.1	<0.1	11.3	45.7±4.5
	29-2, 94-100	26B	Tholeiite	0.985±0.002	0.8078	0.5197	40.8	0.009174	7.426	6.403	0.01630	10.7	0.4	<0.1	42.0	51.1±1.4
	31-1, 7-13	27	Tholeiite	0.450±0.005	0.7536	0.3496	47.2	0.009174	9.526	10.58	0.02245	12.8	0.7	<0.1	39.2	61.2±1.6

^aSubscripts indicate radiogenic (R), calcium-derived (Ca), and potassium-derived (K) argon.
^b $\lambda_K = 0.581 \times 10^{-10} \text{ yr}^{-1}$, $\lambda_{Ca} = 4.962 \times 10^{-10} \text{ yr}^{-1}$, $\lambda_{K/K} = 1.167 \times 10^{-4} \text{ mol/mol}$. Errors are estimates of the standard deviation of precision.
^cCorrected for ³⁷Ar decay, half-life = 37.1 days.

mulas derived by differentiation of the isotope dilution, the ⁴⁰Ar/³⁹Ar, and the relevant age equations (Cox and Dalrymple, 1967; Dalrymple and Lanphere, 1971). Wherever appropriate, weighted means are used where weighting is by the inverse of the estimated variance, rather than simple arithmetic means. The weighting allows age data of different quality to be combined without the poorer data having a disproportional effect on the result. Weighted means are indicated as such in the tables, figures, and discussion.

⁴⁰Ar/³⁹Ar isochrons were calculated using the York 2 least-squares cubic fit with correlated errors (York, 1969), and the formula recommended by York (quoted in Ozima et al., 1977) for the correlation coefficient, *r*. Application of the York 2 fit to ⁴⁰Ar/³⁹Ar data is discussed by Dalrymple and Lanphere (1974).

We have used the new ⁴⁰K decay and abundance constants recommended by the IUGS Subcommittee on Geochronology: $\lambda_{\beta} = 4.962 \times 10^{-10} \text{ yr}^{-1}$, $\lambda_{\epsilon} + \lambda_{\epsilon}' = 0.581 \times 10^{-10} \text{ yr}^{-1}$, $^{40}\text{K}/\text{K} = 1.167 \times 10^{-4}$ (Steiger and Jäger, 1977). In addition, all previously published age data discussed or referenced herein have been converted to the new constants. Because of the logarithmic term in the age equation, the effect of the new constants on calculated ages is not linear. K-Ar ages calculated with the new constants are 2.68 per cent older than those calculated with the old constants at 0.1 m.y., but 1.73 per cent younger at 4500 m.y. In the age range between 0 and 70 m.y., however, the logarithmic effect is small; ages at 70 m.y. calculated with the new constants are 2.54 per cent older than those calculated with the old constants. The reader should keep these effects in mind when comparing the age data in this paper with ages reported in older publications.

Throughout this paper, we use the following conventions. The subscripts R and A (e.g., ⁴⁰Ar_R) refer to radiogenic and atmospheric (nonradiogenic) argon, respectively. The subscripts Ca and K refer to argon isotopes generated by fast-neutron reactions with calcium and potassium. Weighted mean plateau and isochron ages based on the ⁴⁰Ar/³⁶Ar versus ³⁹Ar/³⁶Ar correlation diagram and York 2 fit are indicated by *t_p* and *t_i*, respectively.

K-Ar AGE RESULTS

General Statement

Total Fusion Experiments

The conventional K-Ar and total fusion ⁴⁰Ar/³⁹Ar age data on the 17 samples analyzed are presented in Table 3. Because the samples are altered, these data were obtained to determine minimum ages, to assess the effect of the alteration on the K-Ar system, and to supplement the ⁴⁰Ar/³⁹Ar incremental heating data. Clague et al. (1975) and Dalrymple and Clague (1976) found that ⁴⁰Ar/³⁹Ar total fusion ages on Hawaiian-type whole-rock basalts altered in the submarine environment are frequently consistent with feldspar ages and with ages based on ⁴⁰Ar/³⁹Ar incremental heating experiments, even though the conventional K-Ar ages on

the same rocks are low. They suggested that this may be a consequence of proportional loss (quite possibly at different times and by different mechanisms) of radiogenic ^{40}Ar and K-derived ^{39}Ar from K-bearing clays. Because potassium is measured in the $^{40}\text{Ar}/^{39}\text{Ar}$ technique using ^{39}Ar derived from ^{39}K by a fast-neutron reaction and the ^{39}Ar remaining in the nonretentive clays after a 280°C bake-out is often small or negligible, the $^{40}\text{Ar}/^{39}\text{Ar}$ age commonly approaches or equals the apparent age of the unaltered phases. In contrast, all potassium in the clays is analyzed in the conventional technique, and if the clays do not retain all of their $^{40}\text{Ar}_R$, the conventional K-Ar age is too low. Although this phenomenon has been observed in several studies, cited above, there are no independent criteria by which to evaluate the reliability of the data from individual samples, and the $^{40}\text{Ar}/^{39}\text{Ar}$ total fusion ages should be interpreted cautiously.

The discordances, δ , between the conventional and the $^{40}\text{Ar}/^{39}\text{Ar}$ total fusion ages are shown in Figure 3 as a percentage of the $^{40}\text{Ar}/^{39}\text{Ar}$ ages. As expected for altered rocks, the $^{40}\text{Ar}/^{39}\text{Ar}$ total fusion ages are generally higher (positive δ) than the conventional ages: 11 of the 15 samples have δ values ranging from +2 to +29. It is apparent from the figure that the tholeiitic basalts show the effects of alteration more than the alkalic basalts and the hawaiites, even though several of the tholeiites, particularly those from $\bar{\text{O}}$ jin Flow Unit 5 and Suiko Flow Unit 13, do not appear in thin section to be any more altered than the freshest of the alkalic basalts (Table 1). Another observation from the figure is that the δ value does not always vary with the relative rankings based on thin-section examination (Table 1). Compare, for example, the two samples from $\bar{\text{O}}$ jin Flow Unit 1 (Figure 3). These apparent discrepancies between δ and the petrographic observations suggest that the relative reliability of partially altered K-Ar systems cannot always be determined from thin-section studies alone. In the particular case of the Leg 55 samples, the degree of discordance (δ) also may be misleading if interpreted quantitatively, because of the inhomogeneities introduced by the small (0.5 to 1.0 g) samples used for the conventional Ar analyses and by the uneven distribution of clay minerals within the rocks. Nevertheless, we think that δ is a useful semiquantitative indicator of the effect of the alteration on the K-Ar systems in these samples.

Eight of the Leg 55 alkalic basalt and hawaiite samples have δ values less than +5, and we think that the $^{40}\text{Ar}/^{39}\text{Ar}$ total fusion and conventional K-Ar ages of these are probably quite close to crystallization ages. The δ values of the Leg 55 rocks are notably lower than those for the whole-rock samples from Yūryaku, Daikakuji, and Kimmei seamounts dated by Clague et al. (1975) and Dalrymple and Clague (1976). Five of the seven samples from these seamounts had values between 34 and 53. This comparison indicates that the K-Ar systems in the Leg 55 samples are, in general, less disturbed than other samples that have been successfully dated by $^{40}\text{Ar}/^{39}\text{Ar}$ incremental heating techniques.

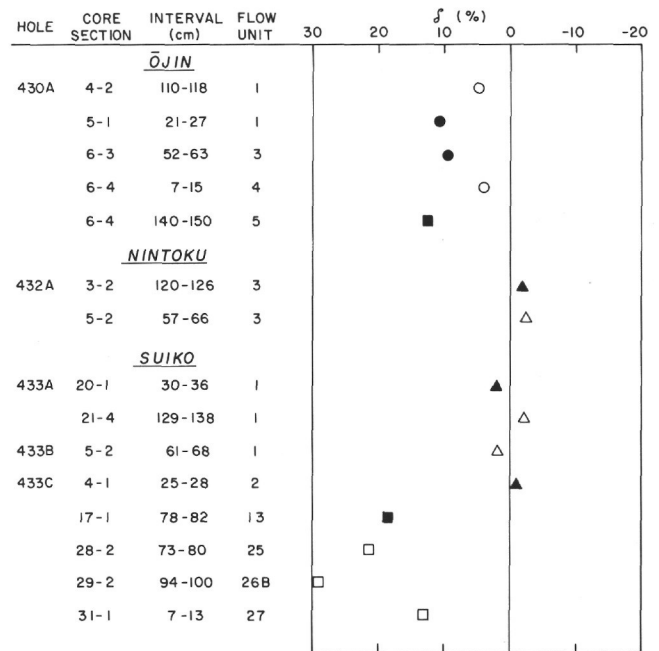


Figure 3. Discordance, δ , between the $^{40}\text{Ar}/^{39}\text{Ar}$ total fusion age and the conventional K-Ar age, expressed as a percentage of the $^{40}\text{Ar}/^{39}\text{Ar}$ total fusion age. Positive values of δ indicate that the $^{40}\text{Ar}/^{39}\text{Ar}$ total fusion age is greater than the conventional K-Ar age. Circles are hawaiites, triangles are alkalic basalts, and squares are tholeiitic basalts. Filled symbols indicate samples for which $^{40}\text{Ar}/^{30}\text{Ar}$ incremental heating data also are available.

Incremental Heating Experiments

$^{40}\text{Ar}/^{39}\text{Ar}$ incremental heating experiments were done on eight samples; the analytical data are presented in Table 4. We have treated the incremental heating data from each sample in two different ways: (1) as an age spectrum or argon-release diagram wherein the apparent age of each gas increment is plotted as a function of the cumulative percentage of the ^{39}Ar released, and (2) as a $^{40}\text{Ar}/^{36}\text{Ar}$ versus $^{39}\text{Ar}/^{36}\text{Ar}$ isochron or correlation diagram, wherein the slope of the line indicates the age of the sample, and the intercept on the ordinate gives the $^{40}\text{Ar}/^{36}\text{Ar}$ composition of nonradiogenic Ar in the sample.

In the age spectrum diagram, we assume that nonradiogenic Ar has the composition of atmospheric Ar ($^{40}\text{Ar}/^{36}\text{Ar} = 295.5$) and calculate an independent age for each gas increment. Interpretation of these diagrams is based on shape, and in the ideal case for an undisturbed sample all the increments will have the same apparent age (Turner, 1968; Dalrymple and Lanphere, 1974). Although interpretation of age spectra from disturbed or altered samples is not always straightforward, it is generally agreed that for igneous rocks a crystallization age may be represented by a plateau, which is a continuous set of gas increments having the same apparent age and representing a significant proportion of the ^{39}Ar released.

TABLE 4
Analytical Data for $^{40}\text{Ar}/^{39}\text{Ar}$ Incremental Heating Experiments on Samples from DSDP Leg 55, Sites 430, 432, and 433

Hole	Core-Section, Interval (cm)	Material	Temp. (°C)	$^{40}\text{Ar}/^{39}\text{Ar}$	$^{37}\text{Ar}/^{39}\text{Ar}_a$	$^{36}\text{Ar}/^{39}\text{Ar}$	^{39}Ar (% of total)	$^{40}\text{Ar}_R$ (%)	$^{36}\text{Ar}_{Ca}$ (%)	Apparent Age ^b (10 ⁶ Years)
ŌJIN SEAMOUNT										
430A	5-1, 21-27	Hawaiite (J=0.009584)	500	8.31	0.775	0.01476	7.5	48.2	1.4	68.0± 2.5
			600	4.071	0.778	0.00287	14.5	80.5	7.4	55.8± 1.0
			700	3.520	1.026	0.00111	36.6	92.9	25.2	55.7± 0.7
			800	3.562	1.354	0.00152	21.4	90.3	24.2	54.8± 0.8
			900	3.746	1.664	0.00224	10.0	85.8	20.2	54.8± 0.9
			975	4.349	2.024	0.00440	4.1	73.7	12.5	54.7± 1.3
			1050	4.543	0.2059	0.00515	4.1	70.0	10.9	54.3± 1.5
			FUSE	7.19	7.42	0.01560	1.8	44.0	12.9	54.3± 4.0
							100.0	Recalculated Total Fusion Age = 56.2± 1.7 Recalculated Total $^{40}\text{Ar}_R/^{39}\text{Ar}_K$ = 3.303 Total $^{40}\text{Ar}_R$ = 1.372×10^{-10} mol/g		
430A	6-3, 52-63	Hawaiite (J=0.006743)	500	40.85	1.004	0.1235	0.8	10.8	0.2	53.2± 14.0
			600	23.03	0.875	0.0607	1.9	22.4	0.4	61.7± 5.0
			700	9.94	0.461	0.01533	5.5	54.8	0.8	65.1± 1.9
			800	7.72	0.844	0.0137	14.5	61.1	2.2	56.5± 1.1
			900	5.93	1.412	0.00466	31.5	78.6	8.2	55.9± 0.9
			975	5.28	0.805	0.00210	15.2	89.3	10.4	56.5± 0.8
			1050	5.38	0.963	0.00265	11.5	86.8	9.9	55.9± 0.8
			FUSE	5.86	4.581	0.00544	19.2	78.8	22.9	55.4± 0.9
							100.1	Recalculated Total Fusion Age = 56.6± 1.7 Recalculated Total $^{40}\text{Ar}_R/^{39}\text{Ar}_K$ = 4.725 Total $^{40}\text{Ar}_R$ = 1.420×10^{-10} mol/g		
430A	6-4, 140-150	Tholeiite (J=0.008220)	500	28.39	1.978	0.0837	22.5	13.4	0.6	55.8± 4.4
			600	25.23	6.49	0.0735	16.3	16.0	2.4	59.1± 4.4
			700	12.48	7.40	0.03121	20.1	30.8	6.4	56.3± 4.3
			800	18.64	7.95	0.0516	13.6	21.6	4.2	59.1± 4.9
			900	20.80	7.69	0.0587	8.4	19.6	3.6	59.7± 7.9
			975	18.07	16.87	0.0523	4.7	22.0	8.8	58.6± 11.3
			1050	13.20	53.0	0.0464	12.0	28.2	31.0	56.3± 6.2
			FUSE	40.3	53.9	0.1402	2.5	8.0	10.5	49.1± 19.2
							100.1	Recalculated Total Fusion Age = 57.2± 1.7 Recalculated Total $^{40}\text{Ar}_R/^{39}\text{Ar}_K$ = 3.921 Total $^{40}\text{Ar}_R$ = 3.04×10^{-11} mol/g		
NINTOKU SEAMOUNT										
432A	2-3, 37-43	Alkalic Basalt (J=0.006743)	500	29.13	0.3945	0.0757	2.0	23.3	0.1	80.6± 8.8
			600	17.41	0.525	0.0353	5.4	40.4	0.4	83.6± 4.0
			700	7.72	0.850	0.01404	8.4	47.1	1.6	43.7± 2.7
			800	5.46	1.017	0.00264	24.1	87.1	10.5	57.0± 0.9
			900	5.08	1.288	0.00210	21.5	89.7	16.7	54.6± 0.8
			975	5.31	1.684	0.00349	11.6	83.0	13.1	52.9± 1.0
			1050	5.15	1.915	0.00302	8.1	85.5	17.2	52.9± 0.9
			FUSE	5.02	2.056	0.00270	19.0	87.3	20.7	52.6± 0.9
							100.1	Recalculated Total Fusion Age = 55.6± 1.7 Recalculated Total $^{40}\text{Ar}_R/^{39}\text{Ar}_K$ = 4.645 Total $^{40}\text{Ar}_R$ = 0.968×10^{-10} mol/g		
432A	3-2, 120-126	Alkalic Basalt (J=0.009584)	500	18.02	1.223	0.0501	3.5	18.3	0.7	56.3± 5.5
			600	9.21	0.838	0.0211	9.3	35.0	1.1	54.9± 2.4
			700	3.815	1.345	0.00214	32.3	86.1	17.1	56.0± 0.8
			800	3.752	1.735	0.00207	20.6	87.3	22.8	55.8± 0.9
			900	3.675	1.554	0.00173	17.1	89.4	24.5	56.0± 0.8
			975	15.41	3.020	0.0405	1.8	24.0	2.0	62.9± 6.4
			1050	5.19	13.45	0.00966	13.0	65.7	37.9	58.5± 1.8
			FUSE	19.31	11.60	0.0573	2.3	17.1	5.5	56.6± 9.3
							99.9	Recalculated Total Fusion Age = 56.3± 1.7 Recalculated Total $^{40}\text{Ar}_R/^{39}\text{Ar}_K$ = 3.309 Total $^{40}\text{Ar}_R$ = 0.981×10^{-10} mol/g		

TABLE 4 — Continued

Hole	Core-Section, Interval (cm)	Material	Temp. (°C)	$^{40}\text{Ar}/^{39}\text{Ar}$	$^{37}\text{Ar}/^{39}\text{Ar}_a$	$^{36}\text{Ar}/^{39}\text{Ar}$	^{39}Ar (% of total)	$^{40}\text{Ar}_R$ (%)	$^{36}\text{Ar}/\text{Ca}$ (%)	Apparent Age ^b (10 ⁶ Years)
SUIKO SEAMOUNT										
433A	20-1, 30-36	Alkalic Basalt (J=0.009063)	500	5.55	1.502	0.00464	9.7	77.4	8.8	69.0± 1.4
			600	8.64	2.316	0.0164	38.6	46.1	3.8	64.0± 1.3
			700	7.62	2.369	0.0132	22.9	51.1	4.9	62.6± 2.3
			800	12.64	1.702	0.0300	11.2	30.8	1.5	62.6± 2.2
			900	25.19	2.211	0.0720	6.1	16.2	0.8	65.6± 4.8
			975	11.61	21.34	0.0325	10.1	31.9	17.8	60.4± 2.3
			1050	39.76	50.31	0.1308	1.2	13.0	10.5	85.0±19.8
			FUSE	158.2	62.94	0.517	0.2	6.6	3.3	171±76
							100.0	Recalculated Total Fusion Age = 64.3± 1.9 Recalculated Total $^{40}\text{Ar}_R/^{39}\text{Ar}_K = 4.001$ Total $^{40}\text{Ar}_R = 0.687 \times 10^{-10}$ mol/g		
433C	4-1, 25-38	Alkalic Basalt (J=0.008220)	500	373.6	2.356	1.207	6.1	4.5	<0.1	236±68
			600	56.1	2.835	0.1685	14.0	11.7	0.5	94.6± 8.5
			700	7.51	2.256	0.1110	43.6	58.7	5.5	64.3± 1.1
			800	11.05	2.003	0.0224	13.8	41.5	2.4	66.9± 1.7
			900	9.38	1.666	0.0176	7.4	46.0	2.6	62.9± 1.9
			975	1.222	16.68	0.0292	12.3	40.3	15.5	72.4± 2.0
			1050	19.35	44.46	0.0579	2.0	30.0	20.9	86.6± 7.7
			FUSE	54.0	62.67	0.1774	0.7	12.3	9.6	99.9±23.8
							99.9	Recalculated Total Fusion Age = 81.5± 9.1 Recalculated Total $^{40}\text{Ar}_R/^{39}\text{Ar}_K = 5.625$ Total $^{40}\text{Ar}_R = 1.000 \times 10^{-10}$ mol/g		
433C	17-1, 78-82	Tholeiite (J=0.008220)	500	12.70	2.842	0.0283	30.2	35.9	2.7	66.4± 2.0
			600	13.65	10.03	0.0335	15.4	33.4	8.2	66.8± 3.6
			700	29.21	11.62	0.0882	33.0	14.0	3.6	59.9± 5.2
			800	13.18	12.65	0.0324	7.9	35.0	10.6	67.8± 4.5
			900	80.60	11.26	0.2618	5.3	5.2	1.2	61.0±12.9
			975	93.79	84.56	0.3246	5.5	5.0	7.1	71.5±15.6
			1050	91.48	119.1	0.3205	2.2	6.9	10.1	98.9±20.3
			FUSE	574.1	100.3	1.924	0.4	2.4	1.4	205±332
							99.9	Recalculated Total Fusion Age = 65.8± 3.5 Recalculated Total $^{40}\text{Ar}_R/^{39}\text{Ar}_K = 4.519$ Total $^{49}\text{Ar}_R = 3.67 \times 10^{-10}$ mol/g		

^a Corrected for ^{37}Ar decay, half-life = 35.1 days.

^b $\lambda_e + \lambda'_e = 0.581 \times 10^{-10} \text{ yr}^{-1}$, $\lambda_\beta = 4.962 \times 10^{-10} \text{ yr}^{-1}$, $^{40}\text{K}/\text{K} = 1.167 \times 10^{-4} \text{ mol/mol}$.
Errors are estimates of the standard deviation of precision.

In the isochron diagram no assumptions are made about the composition of nonradiogenic Ar. After appropriate corrections for interfering Ar isotopes produced in the reactor, the ratio $^{40}\text{Ar}/^{36}\text{Ar}$ is plotted on the ordinate as a function of $^{39}\text{Ar}/^{36}\text{Ar}$ on the abscissa for each gas increment. In the ideal case — i.e., a completely undisturbed and unaltered sample — all the gas increments will lie on a straight line (an isochron) whose slope is the ratio $^{40}\text{Ar}_R/^{39}\text{Ar}_K$, from which the age can be calculated, and whose intercept on the ordinate is 295.5. As in the age spectrum diagram, the interpretation of isochron data for disturbed or altered samples is more complicated, because the points may not all lie on a common line and some judgment must be exercised as to which points to include in the isochron calculations. Another difficulty in interpreting the isochron diagram

for disturbed samples is that the $^{40}\text{Ar}/^{36}\text{Ar}$ intercept may be significantly different from 295.5. Some authors (for example, Jessberger, 1977; Saito and Ozima, 1977) have claimed that such intercepts represent the true composition of the nonradiogenic Ar in the sample and that the isochrons represent valid ages. In contrast, Lanphere and Dalrymple (1978) have shown that non-atmospheric intercepts may simply be a mathematical artifact of an invalid isochron, and that in such cases neither the isochron nor the intercept have geological meaning. Thus, there are two ways to view apparent isochrons with non-atmospheric $^{40}\text{Ar}/^{36}\text{Ar}$ intercepts: (1) as representing valid crystallization ages (Saito and Ozima, 1977), or (2) as an indicator that the isochron data may not be reliable (Lanphere and Dalrymple, 1978). We prefer the second approach because it is

much less likely to lead to incorrect geological conclusions.

To remove as much subjectivity from the interpretation of age spectra and isochrons as possible and to avoid incorrect geological conclusions based on questionable incremental heating data, we have adopted a set of conservative criteria (Lanphere and Dalrymple, 1978) that we will apply to the Leg 55 data. These criteria for an acceptable crystallization age require the following:

1) A well-defined, high-temperature age spectrum plateau formed by three or more contiguous gas increments representing at least 50 per cent of the ^{39}Ar released.

2) A well-defined isochron for the plateau points; i.e., a York 2 fit index ($\text{SUMS}/[\text{N}-2]$) of less than 2.5¹ (Brooks et al., 1972; Dalrymple and Lanphere, 1974).

3) Concordant isochron and plateau ages.

4) An $^{40}\text{Ar}/^{36}\text{Ar}$ intercept on the isochron diagram not significantly different from the atmospheric value of 295.5 at the 95 per cent level of confidence.

Samples that produce data not meeting these criteria are considered too disturbed or altered to yield reliable independent crystallization ages. In addition to applying the above criteria, we have treated the data from each incremental heating experiment using all reasonable combinations of increments (Table 5) in order to determine how critically the calculated plateau and isochron ages are affected by the choice of plateau points.

Ōjin Seamount

Samples from Flow Units 1 and 3, both hawaiites, and from Flow Unit 5, a tholeiitic basalt, were subjected to $^{40}\text{Ar}/^{39}\text{Ar}$ incremental heating experiments with the results shown in Figure 4. All three samples gave age spectra and isochrons that fit the criteria for reliability outlined above. In addition, neither the isochron nor the plateau ages are significantly affected by the choice of which gas increments to exclude from the calculations (Table 5). The results on the tholeiitic basalt are more uncertain than those on the two hawaiites because of the lower percentage of $^{40}\text{Ar}_R$ in the gas increments of the tholeiite (Table 4). Although the plateau and isochron ages for the tholeiitic basalt are numerically older than those for the two hawaiites, the differences are not statistically significant at the 95 per cent level of confidence and the results on all three samples are considered concordant. The incremental heating results are also concordant with the conventional K-Ar and total fusion $^{40}\text{Ar}/^{39}\text{Ar}$ ages of 54.9 to 57.8 m.y. on the two samples from Flow Units 1 and 4 that have δ values less than +5 (Figure 3, Table 3).

We conclude that the plateau and isochron ages from all three samples represent crystallization ages. For the

best age for Ōjin Seamount, we prefer to use the isochron ages because no numerical assumption about the composition of nonradiogenic Ar is required. The weighted mean of the three isochron ages is 55.2 ± 0.7 m.y. If the plateau ages are included in the weighted mean, the result is 55.5 ± 0.6 m.y.

Nintoku Seamount

Of the two samples from Nintoku Seamount for which incremental heating data are available, only the one from Flow Unit 3 gives easily interpreted results (Figure 5). The age spectrum and isochron for this sample (432A-3-2, 120–126 cm) meet all the criteria for a reliable crystallization age. Although the data from the 975°C through fusion increments were omitted from the isochron and weighted mean plateau age calculations because of their high analytical uncertainty, the final result is not sensitive to the exclusion of these points (Table 5).

The sample (432A-2-3, 37–43 cm) from Flow Unit 2 gives an age spectrum in which the apparent age of successive gas increments declines more or less continuously. In addition, the indices of fit ($\text{SUMS}/[\text{N}-2]$) for the isochron using all reasonable combination of points are greater than 2.5, which indicates that the scatter of the data is more than can be accounted for by the analytical uncertainties (Table 5). The errors on the $^{40}\text{Ar}/^{36}\text{Ar}$ intercepts are so large that the intercepts are indeterminate. The data from this sample resemble those reported by Fleck et al. (1977) for altered Mesozoic basalts from Antarctica. They attributed the declining age spectrum in their samples to redistribution without loss of either $^{40}\text{Ar}_R$ during alteration or $^{39}\text{Ar}_K$ by recoil during irradiation (Hueneke and Smith, 1976), or both. It seems likely that some redistribution of Ar has occurred in the Nintoku sample because both the $^{40}\text{Ar}/^{39}\text{Ar}$ total fusion age (56.6 ± 0.8 m.y.; Table 3) and the recalculated total fusion age found by combining the data from the individual increments (55.6 ± 1.7 m.y.; Table 4) are concordant with the crystallization age of the sample from Flow Unit 3.

For the age of Nintoku Seamount, we will use 56.2 ± 0.6 m.y., which is based on the isochron age of the sample from Flow Unit 3 with a slightly more realistic error than is calculated from the York 2 fit. The conventional K-Ar and total fusion $^{40}\text{Ar}/^{39}\text{Ar}$ ages for the two samples (432A-3-2, 120–126 cm and 432A-5-2, 57–66 cm) from Flow 3 both have low δ values (Figure 3) and fall within the range 53.8 to 55.2 m.y. (Table 3). Only the $^{40}\text{Ar}/^{39}\text{Ar}$ total fusion age of the sample from Section 3-2 is significantly different from the age of 56.2 ± 0.6 m.y. at the 95 per cent level of confidence.

Suiko Seamount

The alkalic basalt samples from Flow Unit 1 (433A-20-1, 30–36 cm) and the tholeiitic basalt samples from Flow Unit 13 (433C-17-1, 78–82 cm) both have age spectra and isochrons that meet the criteria for reliable crystallization ages (Figure 6). As was the case with Ōjin Flow Unit 5, the apparent ages of the individual gas increments from the tholeiitic basalt have relatively large

¹ Following Brooks et al. (1972), most authors, including us, have used $(\text{SUMS}/[\text{N}-2])^{1/2}$ as the York 2 equivalent of the mean square of weighted deviates (MSWD) of the McIntyre 1 isochron fit. J. C. Roddick (1978) has pointed out, however, that introduction of the square root term by Brooks et al. (1972) was an error and that the proper equivalency is $\text{MSWD} = \text{SUMS}/(\text{N}-2)$.

TABLE 5
Summary of Age Spectrum and Isochron Analyses of Data from $^{40}\text{Ar}/^{39}\text{Ar}$ Incremental Heating Experiments on Samples from DSDP Leg 55, Sites 430, 432, and 433 (Analyses shown in Figures 4-6 are indicated by asterisks.)

Hole	Core-Section, Interval (cm)	Flow Unit	Rock Type	Increments Used	Age Spectrum		Isochron		
					Wt. Mean Age (10 ⁶ years)	³⁹ Ar (%)	Age (10 ⁶ yrs)	Intercept	SUMS/(N-2)
ŌJIN SEAMOUNT									
430A	5-1, 21-27	1	Hawaiite	All	55.4±0.7	100	54.5±0.7	319±15	3.2
				*600° - Fuse	55.1±0.7	92.5	54.7±0.5	302±12	1.2
				800° - Fuse	54.7±0.9	41.4	54.5±0.6	298±13	0.2
	6-3, 52-63	3	Hawaiite	All	56.4±1.9	100	55.3±0.7	308±8	3.4
				*800° - Fuse	56.0±0.4	77.4	55.6±0.5	303±10	0.9
	6-4, 140-150	5	Tholeiite	*All	57.4±3.5	100	57.6±2.0	295±2	0.2
NINTOKU SEAMOUNT									
432A	2-3, 37-43	2	Alkalic Basalt	All	54.2±2.5	100	52.7±1.4	322±28	15.1
				800° - Fuse	54.1±1.9	60.1	52.7±5.0	332±178	10.3
				*900° - Fuse	53.3±1.0	38.7	55.1±2.4	229±83	2.9
	3-2, 120-126	3	Alkalic Basalt	All	56.1±1.6	100	56.2±0.3	297±4	1.1
				*500°-900°	55.9±1.2	82.9	56.2±0.2	293±2	0.2
SUIKO SEAMOUNT									
433A	20-1, 30-36	1	Alkalic Basalt	All	64.4±9.9	100	64.3±1.9	293±6	4.1
				500°-975°	64.3±1.0	98.6	65.2±2.0	290±7	4.6
				*600°-975°	62.9±1.2	88.9	63.0±1.5	295±5	1.5
433C	4-1, 25-38	2	Alkalic Basalt	All	66±5.8	100	62.8±1.3	309±3	3.4
				*700°-900°	64.7±2.0	64.8	62.2±3.1	308±14	2.5
				700°-975°	65.9±4.0	77.1	59.4±3.6	324±15	4.7
433C	17-1, 78-82	13	Tholeiite	All	66±4.2	100	65.3±1.8	297±2	1.4
				500°-800°	66.1±3.6	86.5	69.9±2.8	288±5	0.1
				500°-900°	66.0±3.6	91.8	67.7±1.9	292±3	0.4
				500°-975°	66.1±3.6	97.3	66.8±1.7	294±2	0.6

uncertainties because of the low percentages of $^{40}\text{Ar}_R$ in the analyses. Also, the isochron and weighted mean plateau ages of the tholeiitic basalt (Flow Unit 13) are numerically greater than those of the alkalic basalt (Flow Unit 1), but the difference is not statistically significant at the 95 per cent level of confidence. The weighted mean of the two isochron ages from Flow Units 1 and 13 is 64.7 ± 1.1 m.y., which we will use as the age of Suiko Seamount. If the plateau ages are included, then the weighted mean is 64.0 ± 1.1 m.y. The data for several gas increments were excluded from the isochron and weighted mean plateau age calculations for Flow Units 1 and 13, but the results are not changed appreciably if some or all of the omitted data are included (Table 5).

The sample (433C-4-1, 25-28 cm) from Flow Unit 2 has a saddle-shaped age spectrum (Figure 6) beginning at 500°C with an apparent age of 236 ± 68 m.y. (off scale on the figure), decreasing to a minimum of 62.9 ± 1.9 m.y. at 900°C, and then increasing steadily in the 975°C through fusion increments to 99.9 ± 23.8 m.y. Lanphere and Dalrymple (1976) have shown that saddle-shaped age spectra are diagnostic of extraneous ^{40}Ar in both igneous minerals and igneous rocks, and that the minima in such spectra are greater than or equal to the crystallization age of the rocks. For this particular sam-

ple, the three gas increments that form the minimum in the age spectrum have a weighted mean age of 64.7 ± 2.0 m.y., which is indistinguishable from the crystallization age indicated by the data from Flow Units 1 and 13. Although not expected, the occurrence of excess ^{40}Ar in the sample of Flow Unit 2 was also unsurprising. Thin-section examination shows that this flow has about 5 per cent of olivine phenocrysts, ranging in size from 0.3 to 3 mm, some of which have well-developed deformation lamellae. These deformed olivines are probably xenocrysts and are a likely source of the excess ^{40}Ar .

The alkalic basalt samples from Suiko all have δ values of +2 or less. The conventional K-Ar and $^{40}\text{Ar}/^{39}\text{Ar}$ total fusion ages on these four samples range only from 59.0 to 63.2 m.y. and have a weighted mean of 60.8 ± 0.4 m.y. This age is significantly lower than the weighted mean isochron age of Flow Units 1 and 13 at the 95 per cent level of confidence, but not statistically different from the ages found by incremental heating for Flow Unit 1 alone. The conventional K-Ar and $^{40}\text{Ar}/^{39}\text{Ar}$ total fusion ages from the tholeiitic basalts are all highly discordant (Figure 3).

DISCUSSION

The new data presented in this paper and from Jingū Seamount by Dalrymple and Garcia (this volume) bring

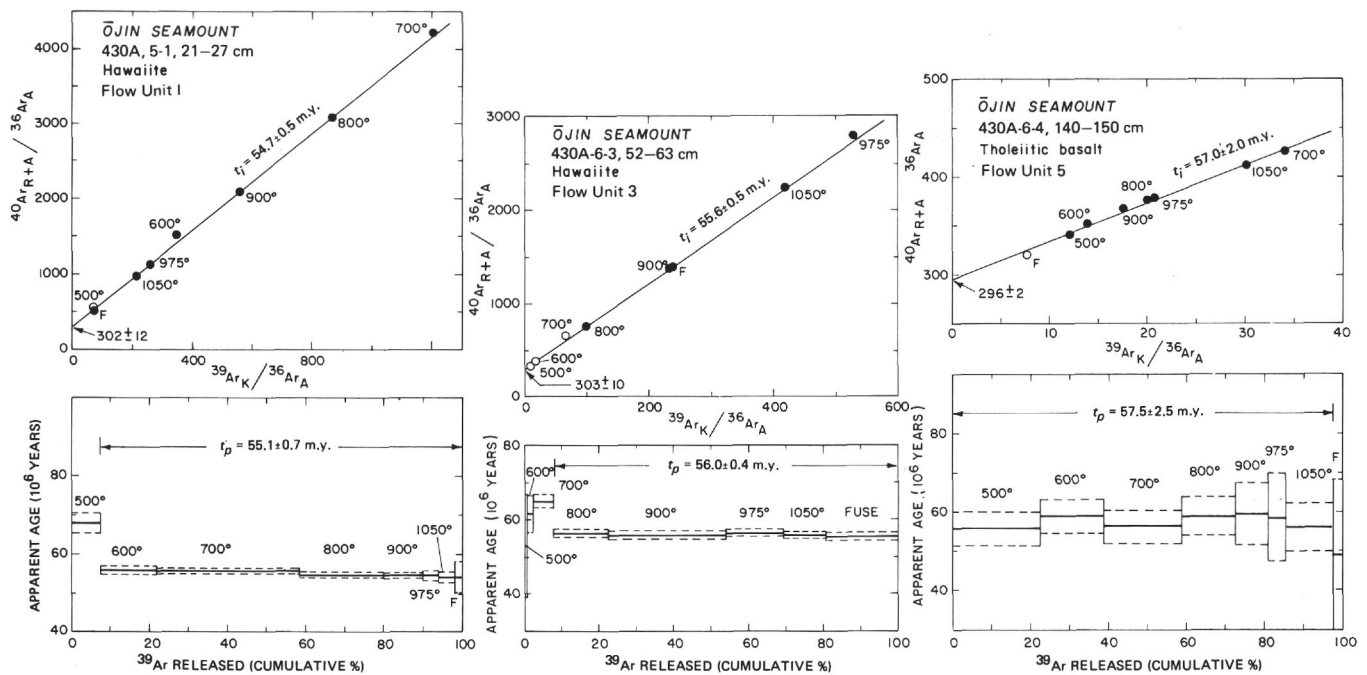


Figure 4. Age spectra and isochron diagrams for $^{40}\text{Ar}/^{39}\text{Ar}$ incremental heating experiments on hawaiite and tholeiitic basalt samples from Ōjīn Seamount. Dashed lines on age spectra indicate the estimated standard deviation of precision about the calculated ages (solid lines) for each gas increment measured. Reliable isochron and weighted mean plateau ages are indicated by t_i and t_p , respectively. Isochron ages are calculated using plateau data, indicated by filled circles. Temperatures are in degrees Celsius.

to 27 the total number of volcanoes in the Hawaiian-Emperor chain for which K-Ar ages have been determined. Of more significance, the age data have now been extended 1275 km northward of the Hawaiian-Emperor bend, or more than halfway up the Emperor Seamount chain. For the first time, there are adequate age data for a definitive test of the kinematic hot-spot hypothesis for both the Hawaiian and the Emperor chains.

The available age data are summarized in Table 6 and plotted in Figure 7 as a function of distance measured from Kilauea Volcano along the Hawaiian-Emperor trend. Because some of the volcanoes are unnamed and some seamounts consist of more than one volcano, each dated volcanic center is identified in the table with the number assigned to it by Bargar and Jackson (1974).

In selecting the age data in Table 6, we have assumed that the volcanoes of the Hawaiian-Emperor chain form by following the same eruptive sequence as do the well-studied volcanoes in the main Hawaiian Islands. The main mass of Hawaiian shield volcanoes is formed by rapid and copious eruptions of tholeiitic basalt. After a brief period of quiescence following caldera formation, a volcano may erupt lavas of the alkalic suite, principally alkalic basalt and hawaiite, which form a thin veneer on the subaerial part of the shield. On Waianae Volcano, this alkalic cap reaches a thickness of more than 700 meters, but the alkalic lavas are still volumetrically a very small proportion (< 1%) of the mass of the shield. After a long period of inactivity and deep erosion, some Hawaiian volcanoes erupt very small amounts of lavas of

the post-erosional or nephelitic suite from satellite cones. These lavas are principally alkalic basalts and nepheline basalts. Some Hawaiian volcanoes become extinct before reaching the post-erosional stage of volcanism.

Ideally, we would like to know the time that each tholeiitic shield volcano first erupted onto the sea floor, but such data clearly are not obtainable. For the principal Hawaiian Islands, McDougall (1971) adopted the approach of using the youngest age of tholeiitic basalt as representing the time of cessation of volcanism for each dated volcano. In contrast, Jackson et al. (1972) used the oldest age obtained for tholeiitic volcanism as the best approximation of the age of the volcanoes. For the summary in Table 6 we have followed the practice of Jackson et al. (1972), but the choice of which ages to use is probably not critical when considering data for the chain as a whole. The reason is that the existing data on the rate of formation of Hawaiian volcanoes indicate that the tholeiitic shields are probably built from the sea floor up in as little as 0.5 to 1.5 m.y. (see summary in Jackson et al., 1972), and this age difference is lost in the analytical uncertainty at about 20 m.y. The question even becomes moot for most of the volcanoes west of Kauai and Niihau because so few suitable samples have been recovered that there is seldom a choice to make.

Most of the age data from islands and seamounts west of La Perouse Pinnacles (French Frigate Shoals) were obtained on rocks of the alkalic suite rather than on tholeiitic basalt. This also probably makes very little difference to the outcome of the hot-spot experiment

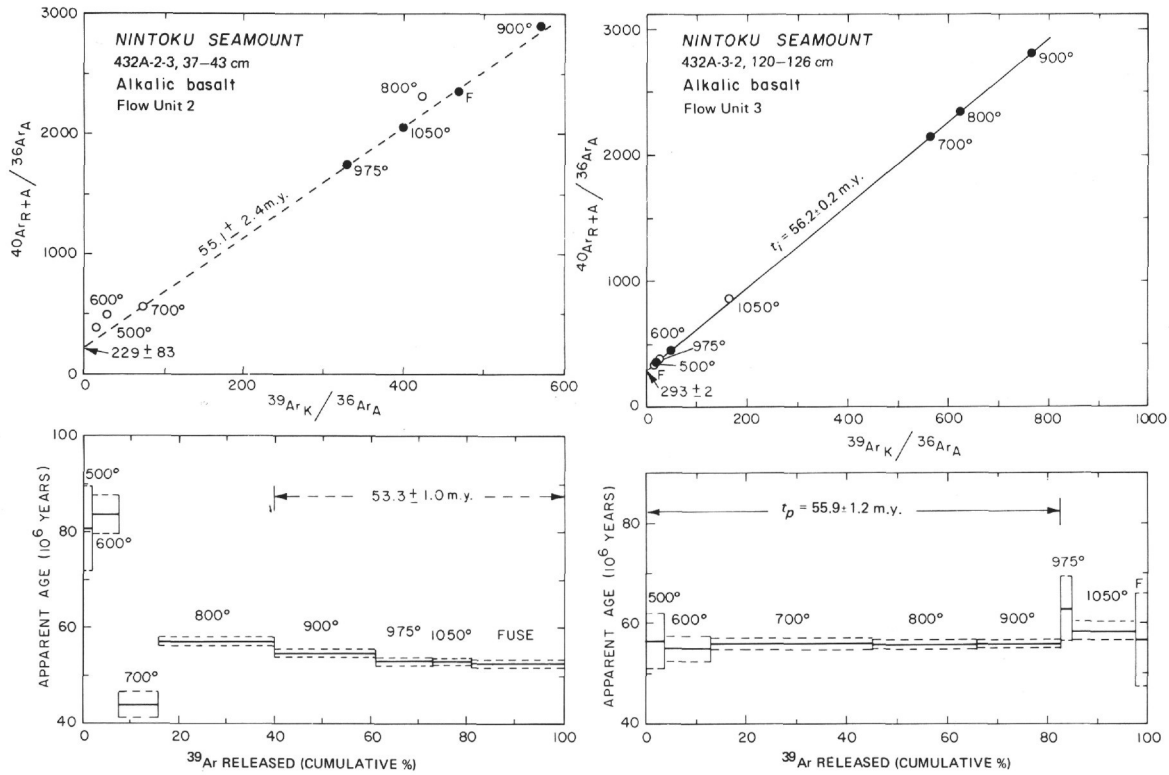


Figure 5. Age spectra and isochron diagrams for $^{40}\text{Ar}/^{39}\text{Ar}$ incremental heating experiments on alkalic basalt samples from Nintoku Seamount. "Plateau" and isochron ages shown for Flow Unit 2 are not considered reliable (see text), and are for reference only. Symbols as in Figure 4.

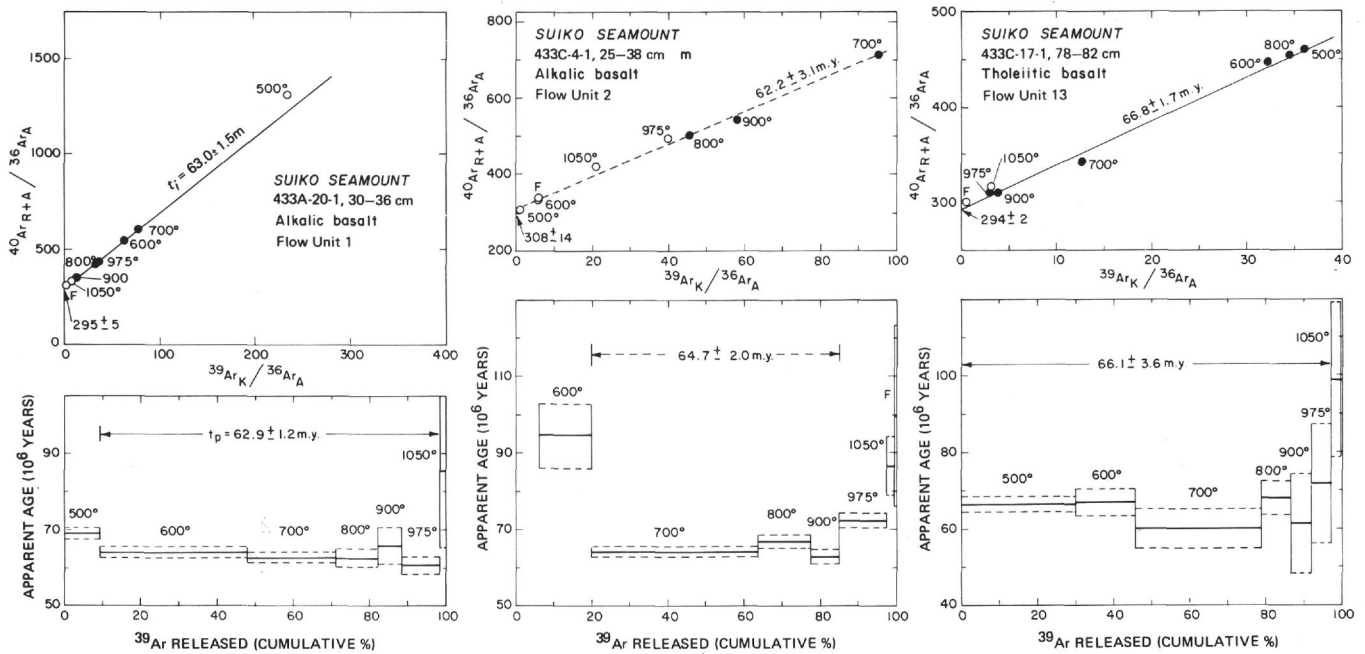


Figure 6. Age spectra and isochron diagrams for $^{40}\text{Ar}/^{39}\text{Ar}$ incremental heating experiments on alkalic and tholeiitic basalt samples from Suiko Seamount. "Plateau" and isochron ages shown for Flow Unit 2 are not considered reliable (see text), and are for reference only. Symbols as in Figure 4.

TABLE 6
Summary of K-Ar Geochronology Along the Hawaiian-Emperor Volcanic Chain

Volcano		Distance From Kilauea Along H-E Trend ^a (km)	Best K-Ar Age ^b (10 ⁶ years)	Reference	Remarks
Name	No. ^a				
Kilauea	1	0	>0 +0.4 -0.0	-	Historic tholeiitic eruptions.
Mauna Kea	3	54	0.375±0.05	Porter et al. (1977)	Samples from tholeiitic shield (Hamakua Group).
Kohala Mtn.	5	100	0.40±0.02	McDougall & Swanson (1972)	Samples from tholeiitic shield (Pololu Volcanic Series).
Haleakala	6	182	0.86±0.03	McDougall (1964)	Age on alkalic basalt (Kula Volcanic Series).
W. Maui	8	221	1.32±0.04	McDougall (1964)	Samples from tholeiitic shield (Wailuku Volcanic Series).
Lanai	9	226	1.28±0.04	Bonhommet et al. (1977)	Samples from tholeiitic shield (Lanai Volcanic Series).
E. Molokai	10	256	1.52±0.05	McDougall (1964)	Samples from tholeiitic shield (lower member of E. Molokai Volcanic Series).
W. Molokai	11	280	1.89±0.06	McDougall (1964)	Sample from tholeiitic shield (W. Molokai Volcanic Series).
Koolau	12	339	2.6±0.1	McDougall (1964); Doell & Dalrymple (1973)	Samples from tholeiitic shield (Koolau Volcanic Series).
Waianae	13	374	3.7±0.1	Doell & Dalrymple (1973)	Samples from tholeiitic shield (lower member, Waianae Volcanic Series).
Kauai	14	519	5.8±0.2	McDougall (1964)	Samples from tholeiitic shield (Napali Formation).
Niihau	15	565	5.5±0.2	Dalrymple (unpublished data)	Samples from tholeiitic shield (Paniau Volcanic Series).
Nihoa	17	780	7.2±0.3	Dalrymple et al. (1974)	Samples from tholeiitic shield.
Necker	23	1058	10.3±0.4	Dalrymple et al. (1974)	Samples from tholeiitic shield.
La Perouse Pinnacle (French Frigates Shoal)	26	1209	12.0±0.4	Dalrymple et al. (1974)	Samples from tholeiitic shield.
Pearl & Hermes Reef	50	2281	20.6±0.5	Clague et al. (1975)	Dredged samples of phonolite, hawaiite, and alkalic basalt.
Midway Islands	52	2432	27.7±0.6	Dalrymple et al. (1977)	Samples of mugearite and hawaiite from conglomerate overlying tholeiitic basalt in drill hole.
Unnamed	57	2600	28.0±0.4	Clague et al. (1975)	Dredged samples of alkalic basalt.
Unnamed	63	2825	27.4±0.5	Clague et al. (1975)	Dredged samples of alkalic basalt, probably from post-erosional suite.
Daikakuji	67	3493	42.4±2.3	Dalrymple & Clague (1976)	Dredged samples of alkalic basalt.
Yūryaku	69	3520	43.4±1.6	Clague et al. (1975)	Dredged samples of alkalic basalt.
Kimmei	72	3668	39.9±1.2	Dalrymple & Clague (1976)	Dredged samples of alkalic basalt.
Kōkō	74	3758	48.1±0.8	Clague & Dalrymple (1973); Dalrymple & Clague (1976)	Dredged samples of alkalic basalt, trachyte, and nepheline phonolite.
Ōjin	81	4102	55.2±0.7	This paper	Samples of hawaiite and tholeiite from DSDP Site 430.
Jingū	83	4175	55.4±0.9	Dalrymple & Garcia (this volume)	Dredged samples of hawaiite and mugearite.
Nintoku	86	4452	56.2±0.6	This paper	Samples of alkalic basalt from DSDP Site 432, probably from alkalic stage.
Suiko	90	4794	59.6±0.6	Saito & Ozima (1975, 1977)	Single dredged sample of mugearite.
	91	4860	64.7±1.1	This paper	Samples of alkalic basalt and tholeiite from DSDP Site 433.

^aFrom Bargar and Jackson (1974) and Bargar, personal communication (1978).

^bAll data have been converted to the new constants $\lambda_e + \lambda'_e = 0.581 \times 10^{-10} \text{ yr}^{-1}$, $\lambda_\beta = 4.962 \times 10^{-10} \text{ yr}^{-1}$, $40\text{K/K} = 1.167 \times 10^{-4} \text{ mol/mol}$.

because the difference between the ages of the alkalic and late-stage tholeiitic suites is only a few hundred thousand years in the Hawaiian Islands (McDougall, 1964, 1969). For one unnamed volcano west of Midway (volcano no. 63) it was necessary to use an age determined from a sample of the nephelinitic suite. On the islands of Oahu and Niihau, the eruption of post-erosional lavas follows the shield-building and alkalic

stages of volcanism by about 2 m.y. (Gramlich et al., 1971) and 5 m.y. (G. B. Dalrymple, unpublished data), respectively, so the main shield of volcano no. 63 may be several million years older than indicated by the K-Ar age in Table 6.

Mineral analyses of pyroxenes in the Leg 55 samples (Clague, Fisk, and Bence, this volume) indicate that the hawaiites from Hole 430A are from the alkalic stage of

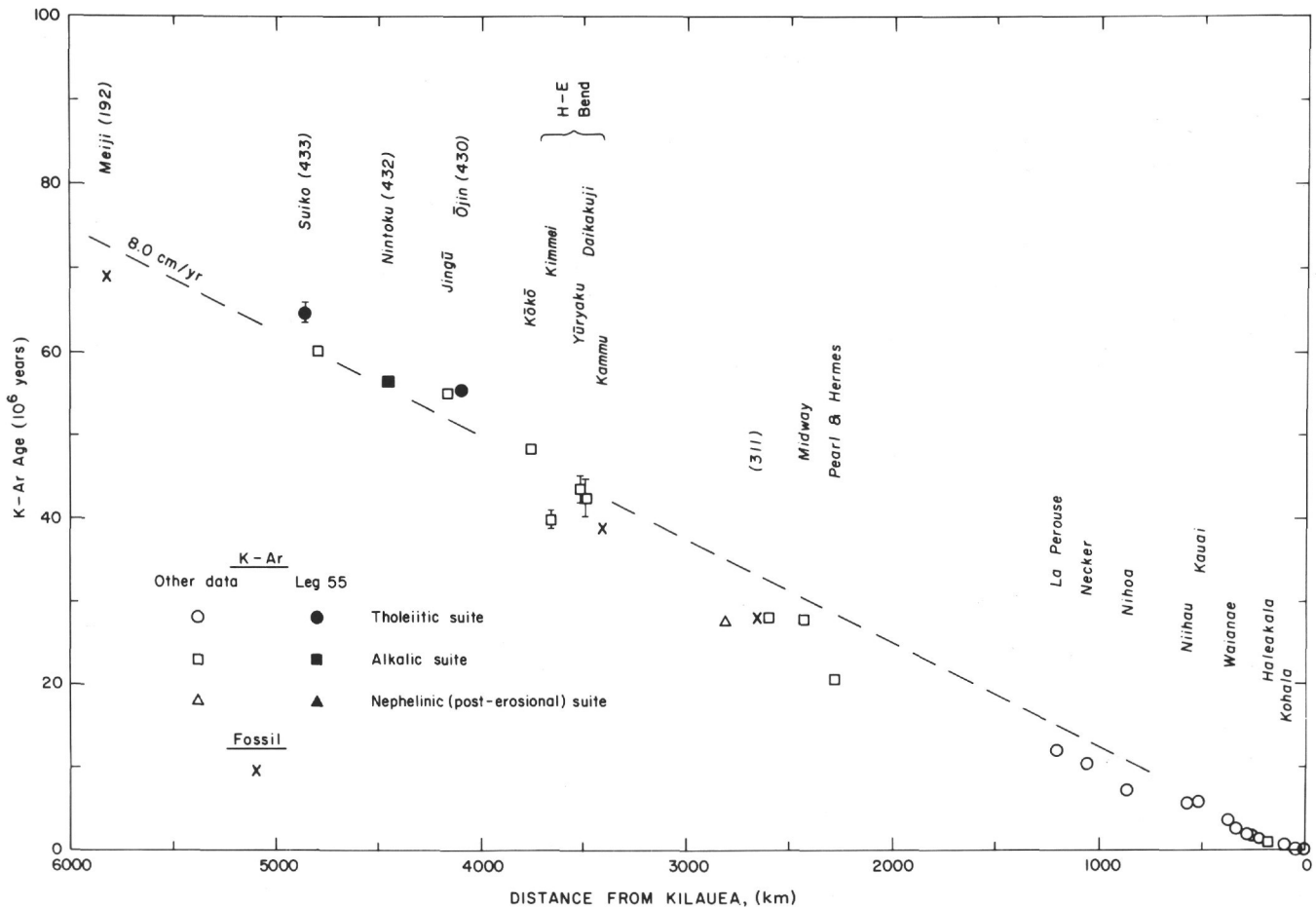


Figure 7. Age of volcanoes in the Hawaiian-Emperor chain as a function of distance from Kilauea Volcano. Errors shown are standard deviations, and are less than symbol size where omitted. K-Ar data from Table 6. Fossil minimum ages are shown only where radiometric data are unavailable (see text). DSDP sites in parentheses.

eruption and that the tholeiite is from the shield-building stage. The alkalic basalts from Hole 432A are probably from the alkalic eruptive stage, although the transitional nature of the pyroxenes does not preclude eruption during the post-erosional stage of eruption. The alkalic basalt flows from Suiko Seamount (Site 433) are from the alkalic stage of eruption, whereas the dated tholeiitic basalts erupted during the shield-building stage. A more complete description of the criteria used to classify the basalts by eruptive stage using pyroxene compositions is given in Clague and Fisk (this volume), Dalrymple and Clague (1976), and Fodor et al. (1975).

The radiometric ages reported by Clague and Dalrymple (1975) for two seamounts on the Hawaiian Ridge have not been listed in Table 6. These include a minimum age of 71 ± 5 m.y. on altered basalt from Wentworth Seamount, 80 km northwest of Midway, and an age of 77.6 ± 1.7 m.y. on a sample of rhyolite dredged from the northern slope of the seamount that underlies Necker Island. These seamounts probably are pre-existing Cretaceous volcanoes that have been overridden by the Hawaiian chain (Clague and Dalrymple, 1975). In addition to these older radiometric data, the Miocene corals and pelagic foraminifers dredged from a

submarine terrace 10 km southwest of Honolulu, Oahu (Menard et al., 1962), and the two samples of Eocene terrigenous sediments recovered 250 km east of Hawaii and 100 km south of Kauai (Schreiber, 1969) may also have originated on volcanoes that predate the Hawaiian chain.

Fossil data have not been included in Table 6, because where both are available, the K-Ar data give the ages of the volcanoes directly. Three minimum ages based on fossil material from seamounts on which radiometric data are unavailable are plotted, however, in Figure 7. These are (1) an age of 28 to 31 m.y. for nanofossils in volcanogenic sediments at DSDP Site 311 on the archipelagic sediment apron of an unnamed seamount (no. 58 of Bargar and Jackson, 1974) 240 km west of Midway (Bukry, 1975), (2) an age of 39 to 41 m.y. for dredged larger foraminifers from Kammu Seamount (Sachs, quoted in Clague and Jarrard, 1973), and (3) an early Maestrichtian date for nanoflora in sediments above basalt in DSDP Hole 192A on Meiji Seamount (Worsley, 1973). Other fossil ages from drill holes on Midway (Cole, 1969; Todd and Low 1970), from DSDP Site 308 on Kōkō Seamount (Bukry, 1975), and from the Leg 55 sites (this volume) on Ōjin, Nin-

toku, and Suiko Seamounts are consistent with the K-Ar data from those volcanoes.

The reliability of the samples and data in Table 6 is adequately discussed in the source references. We wish, however, to comment on the age of 59.6 ± 0.6 m.y. reported by Saito and Ozima (1975, 1977) for a single sample from Suiko Seamount. In addition to the obvious problem of selecting an indigenous sample from the great variety of ice-rafted material dredged from Suiko (Tomoda, 1968), we have reservations about their treatment of the $^{40}\text{Ar}/^{39}\text{Ar}$ incremental heating data. The age they report is based on an $^{40}\text{Ar}/^{36}\text{Ar}$ versus $^{39}\text{Ar}/^{36}\text{Ar}$ isochron with an intercept of 313.6 ± 3.0 and an index of fit (SUMS/[N - 2]) of 3.28. Although the age spectrum they show appears to have a well-defined plateau concordant with the isochron age, the apparent ages of the individual gas increments were calculated using the $^{40}\text{Ar}/^{36}\text{Ar}$ value of 313.6 rather than 295.5 for the nonradiogenic component. As we have pointed out elsewhere (Lanphere and Dalrymple, 1978), unless the sample contains uniformly distributed extraneous ^{40}Ar , this is simply a mathematical device for forcing the age spectrum age to agree with the incorrect isochron age, and may have no geological meaning. When the age spectrum of the Suiko sample is recalculated using a value of 295.5 for $^{40}\text{Ar}/^{36}\text{Ar}$ and the Ar data tabulated by Saito and Ozima (1977), both the concordance and the plateau disappear entirely. Despite our reservations, we cannot exclude the possibility that the age obtained by Saito and Ozima for their Suiko sample is correct. The sample they analyzed was probably recovered from a different volcanic center (Bargar and Jackson, 1974), and an age of 59.6 m.y. does not necessarily conflict with our results from Site 433. Their data do not, however, meet our criteria for reliability, and there are no supporting ages for that volcano. Although we have listed the age in Table 6 and plotted it in Figure 7, we think that it should be interpreted cautiously.

As can be seen from Figure 7, the ages of volcanoes in both the Hawaiian and Emperor chains increase as a function of distance from Kilauea. These data confirm the prediction of the kinematic hot-spot hypothesis for the origin of the chain. The volcanic propagation rate along the chain is about 8 cm/year, but the increase in age with distance is not exactly linear. Several explanations for the deviation from linearity are possible. In addition to analytical errors and the difficulties of working with altered samples, these include, as discussed above, errors caused by dating volcanic rocks that were formed at various stages after inception of the volcanoes. These factors almost invariably result in ages younger than the inception of the volcano. It is also possible that the rate of volcanic propagation is not identical to the relative rate of motion between the Pacific plate and the hot spot, but includes minor changes in velocity as suggested by Jackson et al. (1972) and Shaw (1973). Such changes have been noted for the main Hawaiian Islands, where the velocity of volcanic propagation appears to have accelerated from Kauai to Kilauea (Jackson et al., 1972). We also cannot exclude the possibility of real changes in the rate of relative motion between the hot

spot and the Pacific plate during the last 65 m.y. For example, a velocity of 6.1 cm/year from Suiko to Midway followed by a velocity of 9.2 cm/year from Midway to Kilauea is as consistent with the data as is a constant velocity of 8 cm/year from Suiko to Kilauea. The present data do not, however, allow any major change in the velocity of volcanic propagation at the bend; any reasonable line through the data from Suiko to the bend passes very close to either Kilauea or Midway.

Although there are now K-Ar ages available for most of the Hawaiian-Emperor chain, three major gaps in the data remain. The gap between La Perouse Pinnacles and Pearl and Hermes Reef is entirely due to lack of sampling effort, and can be eventually filled. In fact, samples from the volcanoes that underlie Laysan Island and Northampton Bank, both of which lie about midway in that gap, are now being analyzed (G. B. Dalrymple, D. A. Clague, and M. O. Garcia, unpublished data). The gap east of the bend will never be satisfactorily filled, because there are only two major volcanoes (Colahan and its southern neighbor) between Kammu and the unnamed volcano no. 63. Apparently, the Hawaiian hot spot was relatively inactive between 28 and 42 m.y. ago. The gap north of Suiko will be very difficult to fill unless there is further drilling, because all the seamounts north of Nintoku are covered by a thick blanket of glacial debris. In addition, the weather in the north Pacific provides no small degree of discouragement for those contemplating extensive cruises in that area (Dalrymple, 1977). No doubt future age-dating studies will fill some of these gaps in the data and lead to refined estimates of the volcanic propagation rate along the chain. It seems unlikely, however, that additional data are necessary solely to test the hot-spot hypothesis.

ACKNOWLEDGMENTS

We wish to thank W. B. Friesen and J. Saburomaru for sample preparation, S. E. Sims, B. M. Myers, and J. C. Von Essen for the argon measurements, P. R. Klock for the potassium measurements, and P. G. Helfer and the staff of the U. S. Geological Survey Reactor facility for fast-neutron irradiation of samples. We also appreciate the helpful manuscript reviews of our colleagues R. J. Fleck and H. R. Shaw. We will be forever grateful for the continuing encouragement and inspiration of our friend and colleague, Dale Jackson.

REFERENCES

- Bargar, K. E. and Jackson, E. D., 1974. Calculated volumes of individual shield volcanoes along the Hawaiian-Emperor chain, *U.S. Geol. Survey Jour. of Research*, v. 2, pp. 545-550.
- Bonhommet, N., Beeson, M. H., and Dalrymple, G. B., 1977. A contribution to the geochronology and petrology of the island of Lanai, Hawaii, *Geol. Soc. America Bull.*, v. 88, pp. 1282-1286.
- Brooks, C., Hart, S. R., and Wendt, I., 1972. Realistic use of two-error regression treatments as applied to rubidium-strontium data, *Rev. Geophys. and Space Physics*, v. 10, pp. 551-577.
- Bukry, D., 1975. Coccolith and silicoflagellate stratigraphy, northwestern Pacific Ocean, Deep Sea Drilling Project, Leg 32. In Larson, R. L., Moberly, R., et al., *Initial Reports of*

- the Deep Sea Drilling Project*, v. 32: Washington (U. S. Government Printing Office), pp. 677-701.
- Christofferson, E., 1968. The relationship of sea-floor spreading in the Pacific to the origin of the Emperor Seamounts and the Hawaiian Island chain, *Am. Geophys. Union Trans.*, v. 49, p. 214.
- Clague, D.A. and Dalrymple, G. B., 1973. Age of Kōkō Seamount, Emperor Seamount chain, *Earth Planetary Sci. Letters*, v. 17, pp. 411-415.
- _____, 1975. Cretaceous K-Ar ages of volcanic rocks from the Musicians Seamounts and the Hawaiian Ridge, *Geophys. Research Letters*, v. 2, pp. 305-308.
- Clague, D. A., Dalrymple, G. B., and Moberly, R., 1975. Petrography and K-Ar ages of dredged volcanic rocks from the western Hawaiian Ridge and the southern Emperor Seamount chain, *Geol. Soc. America Bull.*, v. 86, pp. 991-998.
- Clague, D. A. and Jarrard, R. D., 1973. Tertiary Pacific plate motion deduced from the Hawaiian-Emperor chain, *Geol. Soc. America Bull.*, v. 84, pp. 1135-1154.
- Cole, W. S., 1969. Larger foraminifera from deep drill holes on Midway Atoll, *U. S. Geol. Survey Prof. Paper 680-C*, 15 pp.
- Cox, A. and Dalrymple, G. B., 1967. Statistical analysis of geomagnetic reversal data and the precision of potassium-argon dating, *Jour. Geophys. Research*, v. 72, pp. 2603-2614.
- Dalrymple, G. B., 1971. Potassium-argon ages from the Pololu Volcanic Series, Kohala Volcano, Hawaii, *Geol. Soc. America Bull.*, v. 82, pp. 1997-2000.
- _____, 1977. Shipboard observations of a north Pacific storm, *Mariners Weather Log*, v. 21, pp. 302-305.
- Dalrymple, G. B., Alexander, E. C., Jr., Lanphere, M. A., and Kraker, G. P., in press. Irradiation of samples for $^{40}\text{Ar}/^{39}\text{Ar}$ dating using the Geological Survey TRIGA Reactor, *U. S. Geol. Survey Prof. Paper*.
- Dalrymple, G. B. and Clague, D. A., 1976. Age of the Hawaiian-Emperor bend, *Earth Planetary Sci. Letters*, v. 31, pp. 313-329.
- Dalrymple, G. B., Clague, D. A., and Lanphere, M. A., 1977. Revised age for Midway Volcano, Hawaiian volcanic chain, *Earth Planetary Sci. Letters*, v. 37, pp. 107-116.
- Dalrymple, G. B. and Lanphere, M. A., 1969. *Potassium-Argon Dating*. San Francisco (W. H. Freeman and Co.).
- _____, 1971. $^{40}\text{Ar}/^{39}\text{Ar}$ technique of K-Ar dating: A comparison with the conventional technique, *Earth Planetary Sci. Letters*, v. 12, pp. 300-308.
- _____, 1974. $^{40}\text{Ar}/^{39}\text{Ar}$ age spectra of some undisturbed terrestrial samples, *Geochim. Cosmochim. Acta*, v. 38, pp. 715-738.
- Dalrymple, G. B., Lanphere, M. A., and Jackson, E. D., 1974. Contributions to the petrography and geochronology of volcanic rocks from the leeward Hawaiian Islands, *Geol. Soc. America Bull.*, v. 85, pp. 727-738.
- Dana, J. D., 1849. *Geology, Volume 10 of United States Exploring Expedition, During the Years 1838-1839, 1840, 1841, 1842*. Philadelphia (C. Sherman).
- _____, 1890. *Characteristics of Volcanoes*. New York (Dodd, Mead, and Co.).
- Doell, R. R. and Dalrymple, G. B., 1973. Potassium-argon ages and paleomagnetism of the Waianae and Koolau Volcanic Series, Oahu, Hawaii, *Geol. Soc. America Bull.*, v. 84, pp. 1217-1242.
- Fleck, R. J., Sutter, J. F., Elliott, D. H., 1977. Interpretation of discordant $^{40}\text{Ar}/^{39}\text{Ar}$ age-spectra of Mesozoic tholeiites from Antarctica, *Geochim. Cosmochim. Acta*, v. 41, pp. 15-32.
- Fodor, R. V., Keil, K., and Bunch, T. E., 1975. Contributions to the mineral chemistry of Hawaiian rocks, IV. Pyroxenes in rocks from Haleakala and West Maui volcanoes, Maui, Hawaii, *Contrib. Mineral. Petrol.*, v. 50, pp. 173-195.
- Funkhouser, J. G., Barnes, I. L., and Naughton, J. J., 1968. The determination of a series of ages of Hawaiian volcanoes by the potassium-argon method, *Pacific Sci.*, v. 22, pp. 369-372.
- Gramlich, J. W., Lewis, V. A., and Naughton, J. J., 1971. Potassium-argon dating of Holocene basalts of the Honolulu Volcanic Series, *Geol. Soc. America Bull.*, v. 82, pp. 1399-1404.
- Hinds, N. E. A., 1931. The relative age of the Hawaiian landscapes, *Univ. California Dept. Geol. Sci. Bull.*, v. 20, pp. 143-260.
- Hunke, J. C. and Smith, S. P., 1976. The realities of recoil: ^{39}Ar recoil out of small grains and anomalous age patterns in ^{39}Ar - ^{40}Ar dating, *Proc. Lunar Sci. Conference, 7th*, pp. 1987-2008.
- Ingamells, C. O., 1970. Lithium metaborate flux in silicate analysis, *Anal. Chim. Acta*, v. 52, pp. 323-334.
- Jackson, E. D., 1976. Linear volcanic chains on the Pacific plate. In Sutton, G. H., Manghnani, M. H., and Moberly, R. (Ed.), *The Geophysics of the Pacific Ocean Basin and its Margin: Am. Geophys. Union Geophys. Mon. 19*, pp. 319-335.
- Jackson, E. D., Shaw, H. R., and Bargar, K. E., 1975. Calculated geochronology and stress field orientations along the Hawaiian chain, *Earth Planetary Sci. Letters*, v. 26, pp. 145-155.
- Jackson, E. D., Silver, E. A., and Dalrymple, G. B., 1972. Hawaiian-Emperor chain and its relation to Cenozoic circum-Pacific tectonics, *Geol. Soc. America Bull.*, v. 83, pp. 601-618.
- Jarrard, R. D. and Clague, D. A., 1977. Implications of Pacific Island and seamount ages for the origin of volcanic chains, *Rev. Geophys. and Space Physics*, v. 15, pp. 57-76.
- Jessberger, E. K., 1977. Comment on "Identification of excess ^{40}Ar by the $^{40}\text{Ar}/^{39}\text{Ar}$ age spectrum technique" by M. A. Lanphere and G. B. Dalrymple, *Earth Planetary Sci. Letters*, v. 37, pp. 167-168.
- Lanphere, M. A. and Dalrymple, G. B., 1971. A test of the $^{40}\text{Ar}/^{39}\text{Ar}$ age spectrum technique on some terrestrial materials, *Earth Planetary Sci. Letters*, v. 12, pp. 359-372.
- _____, 1976. Identification of excess ^{40}Ar by the $^{40}\text{Ar}/^{39}\text{Ar}$ age spectrum technique, *Earth Planetary Sci. Letters*, v. 32, pp. 141-148.
- _____, 1978. The use of $^{40}\text{Ar}/^{39}\text{Ar}$ data in evaluation of disturbed K-Ar systems. In Zartman, R. E., (Ed.), *Short Papers of the Fourth International Conference, Geochronology, Cosmochronology, Isotope Geology: U. S. Geol. Survey Open-File Report 78-701*, pp. 241-243.
- McDougall, I., 1963. Potassium-argon ages from western Oahu, Hawaii, *Nature*, v. 197, pp. 344-345.
- _____, 1964. Potassium-argon ages from lavas of the Hawaiian Islands, *Geol. Soc. America Bull.*, v. 75, pp. 107-128.
- _____, 1969. Potassium-argon ages on lavas of Kohala Volcano, Hawaii, *Geol. Soc. America Bull.*, v. 80, pp. 2597-2600.
- _____, 1971. Volcanic island chains and sea-floor spreading, *Nature*, v. 231, pp. 141-144.
- McDougall, I. and Swanson, D. A., 1972. Potassium-argon ages of lavas from the Hawi and Pololu Volcanic Series, Kohala Volcano, Hawaii, *Geol. Soc. America Bull.*, v. 83, pp. 3731-3738.

- Mankinen, E. A. and Dalrymple, G. B., 1972. Electron microprobe evaluation of terrestrial basalts for whole-rock K-Ar dating, *Earth Planetary Sci. Letters*, v. 17, pp. 89-94.
- Menard, H. W., Allison, E. C., and Durham, J. W., 1962. A drowned Miocene terrace in the Hawaiian Islands, *Science*, v. 138, pp. 896-897.
- Morgan, W. J., 1972a. Deep mantle convection plumes and plate motions, *Am. Assoc. Petroleum Geologists Bull.*, v. 56, pp. 203-213.
- _____, 1972b. Plate motions and deep mantle convection. In Shagam, R., et al., (Ed.), *Studies in Earth and Space Sciences: Geol. Soc. America Mem. 132 (Hess Volume)*, pp. 7-22.
- Ozima, M., Honda, M., and Saito, K., 1977. ^{40}Ar - ^{39}Ar ages of guyots in the western Pacific and discussion of their evolution, *Royal Astron. Soc. Geophys. Jour.*, v. 51, pp. 475-485.
- Ozima, M., Kaneoka, I., and Aramaki, S., 1970. K-Ar ages of submarine basalts dredged from seamounts in the western Pacific area and discussion of oceanic crust, *Earth Planet. Sci. Letters*, v. 8, pp. 237-249.
- Porter, S. C., Stuiver, M., and Yang, I. C., 1977. Chronology of Hawaiian glaciations, *Science*, v. 195, pp. 61-63.
- Roddick, J. C., 1978. The application of isochron diagrams in ^{40}Ar - ^{39}Ar dating: A discussion, *Earth and Planetary Sci. Letters*, pp. 233-244.
- Saito, K. and Ozima, M., 1975. ^{40}Ar - ^{39}Ar isochron age of a mugarite dredged from Suiko Seamount in the Emperor chain, *Rock Magnetism and Paleogeophysics*, v. 3, pp. 81-84.
- _____, 1977. ^{40}Ar - ^{39}Ar geochronological studies on submarine rocks from the western Pacific area, *Earth Planetary Sci. Letters*, v. 33, pp. 353-369.
- Schreiber, B. C., 1969. New evidence concerning the age of the Hawaiian Ridge, *Geol. Soc. American Bull.*, v. 80, pp. 2601-2604.
- Shaw, H. R., 1973. Mantle convection and volcanic periodicity in the Pacific: Evidence from Hawaii, *Geol. Soc. America Bull.*, v. 84, pp. 1505-1526.
- Sherrill, N. D. and Dalrymple, G. B., in press. A computerized multichannel data acquisition and control system for high-precision mass spectrometry, *U. S. Geol. Survey Prof. Paper 1129A*.
- Stacey, J. S., Sherrill, N. D., Dalrymple, G. B., Lanphere, M. A., and Carpenter, N. V., 1978. A computer-controlled, five-collector mass spectrometer for precision measurement of argon isotope ratios. In Zartman, R. E., (Ed.), *Short Papers of the Fourth International Conference, Geochronology, Cosmochronology, Isotope Geology: U. S. Geol. Survey Open-file Report 78-701*, pp. 411-413.
- Stearns, H. T., 1946. *Geology of the Hawaiian Islands, Hawaii Div. of Hydrography Bull.* 8, 106 pp.
- Steiger, R. H. and Jäger, E., 1977. Subcommission on geochronology: Convention on the use of decay constants in geo- and cosmochronology, *Earth Planetary Sci. Letters*, v. 36, pp. 359-362.
- Todd, R. and Low, D. 1970. Smaller foraminifera from Midway drill holes, *U. S. Geol. Survey Prof. Paper 680-E*, 46 pp.
- Tomoda, Y., 1968. *Preliminary Report of the Hakuho Maru Cruise KH-68-3*, Ocean Research Institute, Univ. Tokyo, 116 pp.
- Turner, G., 1968. The distribution of potassium and argon in chondrites. In Ahrens, L. H., (Ed.), *Origin and Distribution of the Elements*: New York (Pergamon Press).
- Wentworth, C. K., 1927. Estimates of marine and fluvial erosion in Hawaii, *Jour. Geology*, v. 35, pp. 117-133.
- Wilson, J. T., 1963a. Evidence from islands on the spreading of ocean floors, *Nature*, v. 197, pp. 536-538.
- _____, 1963b. A possible origin of the Hawaiian Islands, *Canadian Jour. Physics*, v. 41, pp. 863-870.
- Worsley, J. R., 1973. Calcareous nannofossils: Leg 19 of the Deep Sea Drilling Project. In Creager, J. S., Scholl D. W., et al., *Initial Reports of the Deep Sea Drilling Project*, v. 19: Washington (U. S. Government Printing Office), pp. 741-750.
- Yanase, Y., Wampler, J. M., and Dooley, R. E., 1975. Recoil-induced loss of ^{39}Ar from glauconite and other clay minerals (abs.), *EOS (Am. Geophys. Union Trans.)*, v. 56, p. 472.
- York, D., 1969. Least squares fitting of a straight line with correlated errors, *Earth Planetary Sci. Letters*, v. 5, pp. 320-324.